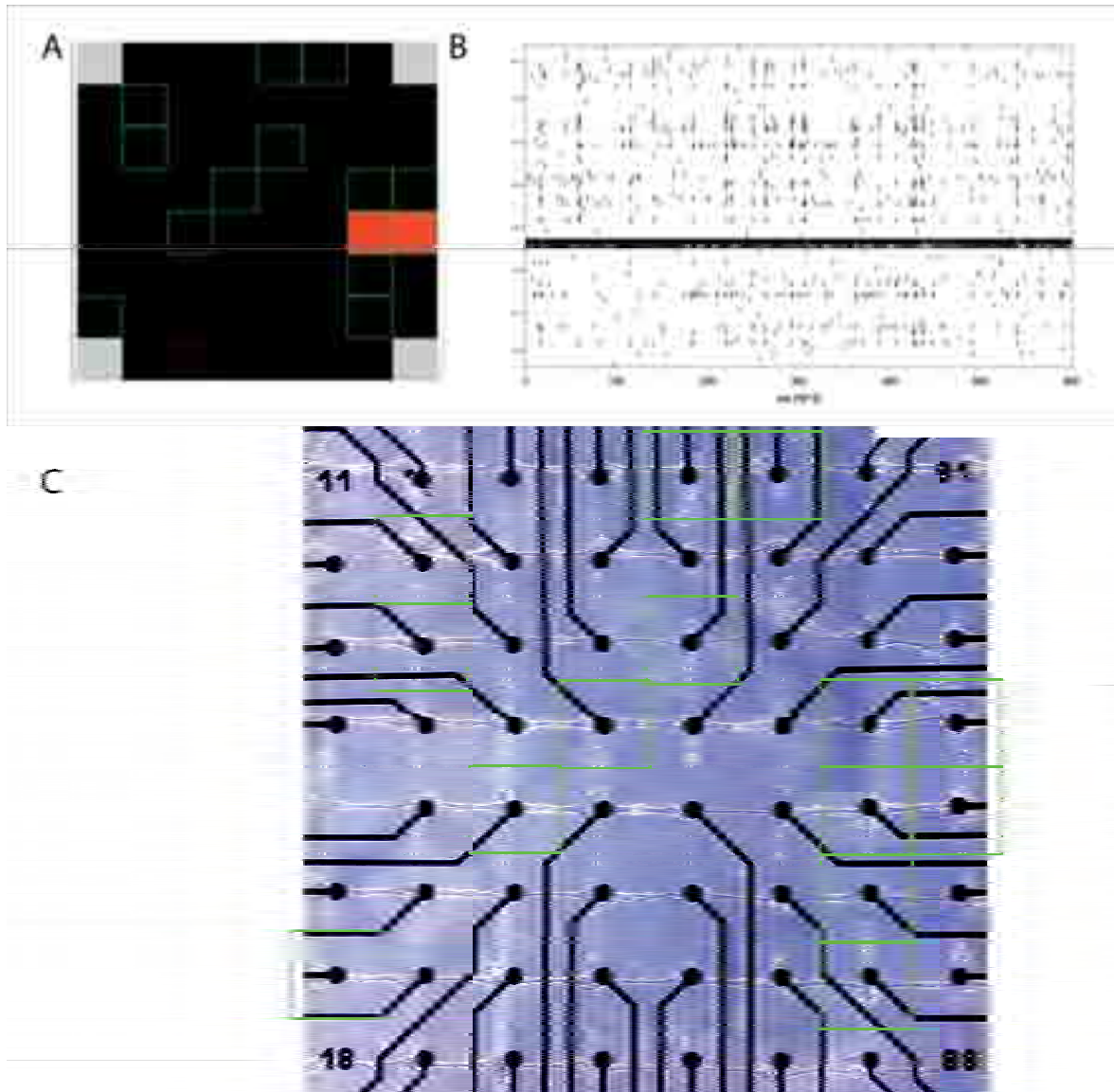


investigating the relationships between network geometry and functional connections.



**Fig. 1** Representative neuronal culture grown on micro-printed MEA (14 DIVs), E18 Rat hippocampal neurons. Extracellular electrical activity was recorded in low cell density culture conditions (70 cells/mm<sup>2</sup>). Both morphological and functional features were maintained despite the bounding conditions. A) MEA Activity Map reports the active channels in the green square (Firing rate > 0.1 spike/sec). B) Raster plot of MEA. Synchronization starts to show up at DIV14. C) Image of the MEA with neuronal cultures aligned on the electrode grid. The active channels are reported as green squares.

# Network Activity Patterns in the Subthalamic Nucleus of the Rat

Jan Stegenga<sup>1\*</sup>, Richard van Wezel<sup>1</sup>, Tjitske Heida<sup>1</sup>

<sup>1</sup> Mira institute of biomedical technology, Biomedical signals and systems group, University of Twente, Enschede, The Netherlands

\* Corresponding author. E-mail address: j.stegenga@utwente.nl

In Parkinson's Disease, pacemaker-like stimulation of the Subthalamic Nucleus (STN) at a frequency near 130 Hz can suppress symptoms like tremor, rigidity and bradykinesia. However, the mechanism by which this so-called Deep Brain Stimulation (DBS) exerts its effect is unknown. In order to increase our understanding of the network in which the STN is involved (the basal ganglia, among others involved in motor tasks), we are now measuring neuronal activity in brain slices containing STN using 3D-MEAs. 3D-MEAs offer the possibility to measure a large number of sites simultaneously in slices which retain *in-vivo* topography and connectivity. This approach is not yet used within Parkinson's Disease research and may answer crucial questions about the (patho-) physiology of the STN and surrounding network.

## 1 Introduction

The symptoms of Parkinson's disease (a.o. muscle rigidity, tremor, bradykinesia) can be suppressed by electrical stimulation of the basal ganglia [1]. The most common target nucleus of this so called Deep Brain Stimulation (DBS) is the subthalamic nucleus (STN). The mechanism(s) responsible for the clinical improvements through DBS are not yet elucidated. Based on organotypic culture studies, many models incorporate synchronous oscillatory activity between STN and external segment of the globus pallidus (GPe) [2]. This, in turn, would disrupt the functioning of the basal ganglia output structures (thalamus, globus pallidus internal internus (GPi); see figure 1). To date, such oscillations have not been observed *in-vivo*. Increasing complexity of models of the basal ganglia involve changes not only in firing rate, but also in oscillatory behavior and synchronous firing [3].

The location of the STN necessitates invasive methods in order to measure activity *in-vivo*. As such, activity is mostly measured at a single site and it is difficult to relate the activity in one nucleus to activity in another nucleus. As part of the BrainGain project, we study rat midbrain slices by means of multi electrode arrays. We will describe results on the relationships between firing patterns of neurons throughout the STN during spontaneous activity. In addition, activity may be evoked by pulses on an electrode, either from the array or from a separate microelectrode. Spatio-temporal responses to single pulses and high-frequency trains of pulses are studied.

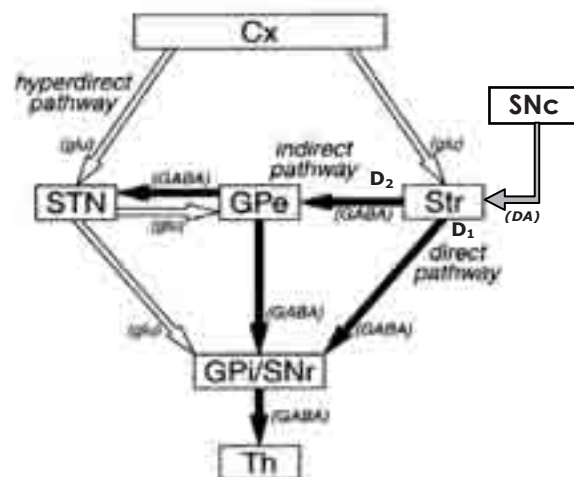
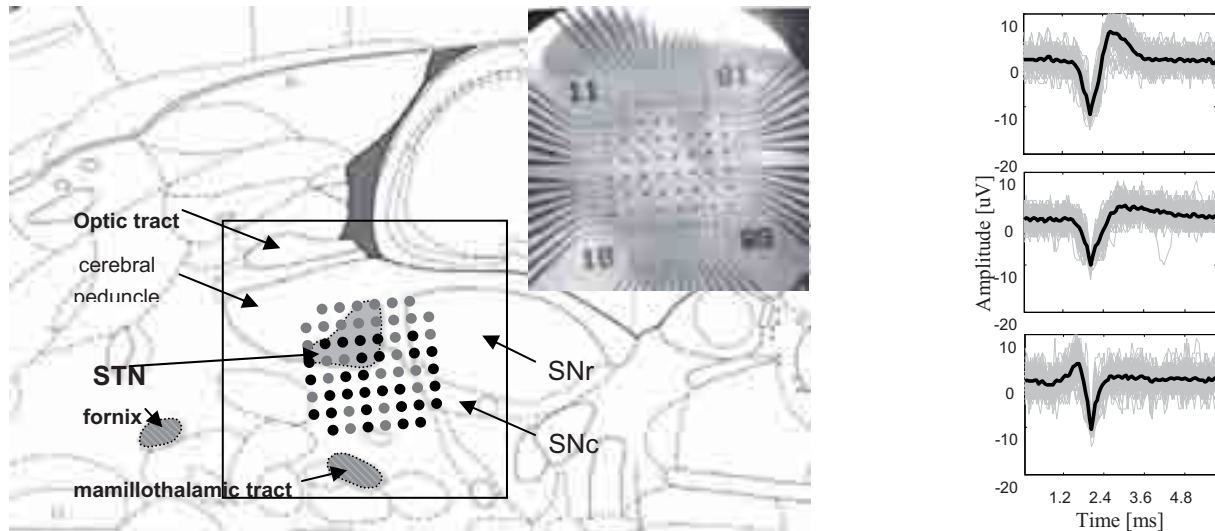


Fig. 1. Schematic of the main connectivity in the Basal Ganglia. The effect of dopaminergic innervation (DA) of the striatum (Str) depends on the receptor type: D<sub>1</sub>-dopamine receptors are excitatory, while D<sub>2</sub> receptors are inhibitory. Other neurotransmitters are always excitatory (Glutamate, Glu) or inhibitory (gamma-amino butyric acid, GABA). Cx=cortex, SNc/r=substantia nigra pars compacta/reticulata. Adapted from Nambu et al. [4]

## 2 Methods

### 2.1 Slice preparation

Coronal brain slices (300  $\mu\text{m}$ ) from 16-52 day-old Wistar rats were cut on a Vibratome (Leica VT1000) in an ice-cold cutting medium containing artificial cerebro-spinal fluid (aCSF) with additional  $\text{MgSO}_4$  and ascorbic acid. Solutions were aerated with carbogen. Rats were anaesthetized using Isoflurane before decapitation.



**Fig. 2.** (left) A MEA superimposed on the corresponding figure of the brain atlas (187, Paxinos & Watson, 2007). Some of the structures used for reference are indicated. Active electrodes are drawn in black. The inset shows a picture of the slice on the MEA. The optic tract, cerebral peduncle and mamillothalamic tract appear dark. (Right) Three examples of action-potential wave forms.

## 2.2 Recording setup

Slices and aCSF were transferred to 3D-multi electrode arrays (3D-MEA; Ayuda biosystems), and signals were amplified, bandpass filtered (10 Hz-10 kHz) and digitized using a setup by MultiChannelSystems. Slices were kept in place by a nylon mesh glued onto a silver ring, lowered into the chamber by a micromanipulator and perfused with aerated aCSF at a rate of  $\sim 3$  ml/min. Signals were visualized by a custom-made LabView program and threshold crossings exceeding 5 times the RMS noise value (typically 2 to 3  $\mu$ V) were stored. Measurements were carried out at room temperature.

## 3 Results

We were able to record action-potential activity from many electrodes located within the midbrain (figure 2). We compared the location of the slice to the brain atlas (Paxinos and Watson, 2007) to identify which electrodes we recorded from were located in STN. Electrodes corresponding to STN, SNr, SNc or PLH (peduncular part of lateral hypothalamus, medial to STN and CP in figure 2) are sometimes active, while electrodes in the cerebral peduncle generally are not. The rate of firing responds to bath application of L-glutamine, potassium and magnesium thus proving their biological origin.

## 4 Conclusions

Recordings with multi electrode arrays can contribute to solving important questions in Parkinson disease research and also to improve our understanding of other neurological disorders. Specialized multi-electrode arrays can be designed for

a specific target, thus increasing the applicability even further.

### Acknowledgement

We thank Irina I. Stoyanova and Geert M. J. Ramakers for practical and scientific contributions and Bettie Klomphaar for preparation of slices.

### References

- [1] Lozano, A.M. (2001), Deep brain stimulation for Parkinson's disease. *Parkinsonism Relat Disord*, 7(3), 199-203.
- [2] Plenz, D., Kital, S.T. (1999), A basal ganglia pacemaker formed by the subthalamic nucleus and external globus pallidus. *Nature*, 400(6745), 677-682.
- [3] Cagnan, H., Meijer, H.G., van Gils, S.A., Krupa, M., Heida, T., Rudolph, M., Wadman, W.J., Martens, H.C. (2009), Frequency-selectivity of a thalamocortical relay neuron during Parkinson's disease and deep brain stimulation: a computational study. *Eur J Neurosci* 30(7), 1306-1317.
- [4] Nambu, A., Tokuno, H., Takada, M. (2002), Functional significance of the cortico-subthalamo-pallidal 'hyperdirect' pathway. *Neurosci Res*, 43(2), 111-117.

# How to Reduce Stimulus/Response Variability in Cortical Neuronal Networks

Oliver Weihberger<sup>1,2,3\*</sup>, Samora Okujeni<sup>1,2,3</sup>, Ulrich Egert<sup>1,3</sup>

1 Bernstein Center for Computational Neuroscience Freiburg

2 Faculty of Biology

3 IMTEK - Department of Microsystems Engineering  
University of Freiburg, Freiburg, Germany

\* Corresponding author. E-mail address: weihberger@bccn.uni-freiburg.de

Repeated application of the same electrical or sensory stimulus evokes varying responses in neuronal networks. Independent of top-down influences such as behavior, attention or conscious state, this can be attributed to interactions between ongoing and evoked activity. The state of the network at the moment of stimulation critically determines over the evoked response. The goal of this study was to identify low-level mechanisms that underlie the modulation of stimulus/response relations. We aimed for predictive models and reproducible responses in targeted interaction with neuronal network activity.

## 1 Introduction

One of the most astonishing features of the central nervous system is its functional power in spite of its variability – the same stimulus elicits different responses in repeated trials. Our behavior, attention or conscious state alters the way external stimuli are processed and information is represented. While learning represents a directed, long-term modification of stimulus/response relations, undirected changes on shorter time scales were ascribed to interactions between ongoing and evoked activity.

Various means were used to describe this interrelation. In general, low levels of pre-stimulus activity led to stronger responses and shorter delays [1-3]. The identification of precise functional relations and the coupling to ongoing spiking activity deserves a closer study.

Understanding the mechanisms of stimulus/response modulation becomes increasingly important for neurotechnological applications. A reliable operation of e.g. visual or auditory cortical implants requires to feed defined patterns of activity into the dynamics of ongoing activity.

We recorded and stimulated cortical cell cultures on microelectrode arrays (MEAs). Electrical stimuli were placed randomly in between periods of synchronous network-wide bursting. User-defined interaction with network activity controlled the stimulus timing relative to ongoing bursting activity. Stimuli were placed at pre-defined states of network inactivity. This enhanced response reproducibility and facilitated the examination of state-dependent input/output relations.

## 2 Material and Methods

### 2.1 Cell culture preparation

Cells from prefrontal cortical tissue of neonatal wistar rats were cultured on polyethylene imine-coated MEAs. Cultures were maintained in MEM supplemented with heat-inactivated horse serum (5%), L-glutamine (0.5 mM), and glucose (20 mM) at 37° C and 5% CO<sub>2</sub>. Medium was partially replaced twice per week.

### 2.2 Recording and stimulation

A Multi Channel Systems MEA1060BC amplifier, STG2008 stimulus generator and MeaBench [4] were used for recording and stimulation inside the incubator. Monophasic negative voltage pulses, width 400  $\mu$ s, amplitudes  $\geq 0.4$  Volt were used. Stimuli were triggered either *i*) at fixed inter-stimulus intervals (IstimI) of 10 or 20 sec., or *ii*) after a defined period without spike (post-burst interval) from a selected feedback site has passed. A minimum IstimI of 10 sec. was enforced.

## 3 Results

### 3.1 Response delays decreased with longer duration of pre-stimulus inactivity

The duration of pre-stimulus inactivity modulated response delays. Long periods of inactivity led to small delays. Bursting activity prior to stimulation led to large delays. Millisecond response delays were determined by the pre-stimulus activity on a time scale of seconds (Fig. 1).

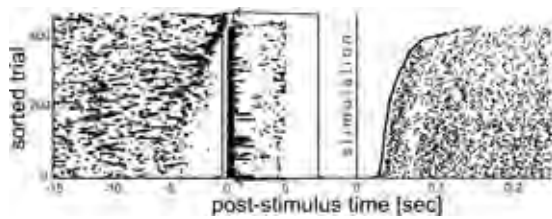


**Fig. 1.** left: raster plot, recording site 22. 471 stimuli with 20 sec. Isimf applied at site 67. Trials were sorted for increasing response delay. right: zoom in around stimulation. Note the increasing delays from  $\approx 25$ ms to  $\approx 125$  ms and the corresponding arrangement of pre-stimulus activity.

### 3.2 Control of stimulus timing enhanced response reproducibility

Post-burst stimulation controlled the timing of stimulation relative to ongoing activity. Responses became more regular. Response variability (standard deviation (std) of response length normalized by the std of spontaneous burst length) decreased. Single-site reliability (no. responses / no. trials) increased compared to fixed-interval stimulation (Fig. 2).

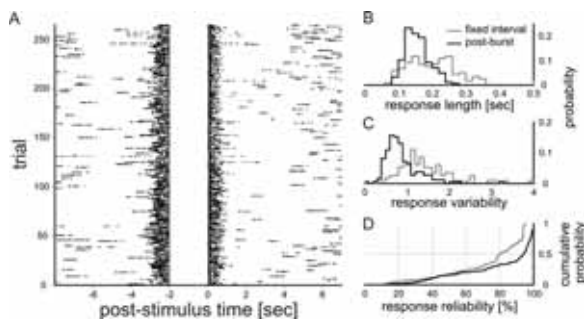


**Fig. 2.** Post-burst stimulation **A**, raster plot, recording site 14. Pre-stimulus bursts terminated at the same time. The state of the network was comparable in each trial. **B-D**, Statistical comparison to fixed-interval stimulation. Responses were shorter and more narrowly distributed (**B**), Response variability decreased (**C**), reliability increased (**D**). 119 (fixed-interval) resp. 185 recording sites with 1, 1.5 or 2 sec. post-burst interval were analyzed.

### 3.3 Network-state dependent propagation speed

Post-burst stimulation facilitated a controlled examination of state-dependent stimulus/response relations. Response delays increased with distance to stimulation site. That is, the initial focus of activation propagated from the site of stimulation. Propagation paths were independent of the network state. Propagation speed, however, was faster for longer pre-stimulus inactivity (Fig. 3).

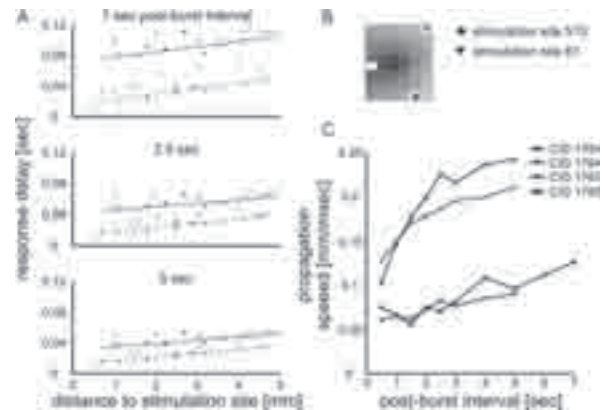


**Fig. 3.** **A, B**, Stimulation with 8 different post-burst intervals at two different sites. Approx. 250 trials in each case (**B**). Response delays increased with the distance to stimulation site. The direction of propagation was maintained (**A**). **C**, Propagation speeds increased with longer duration of pre-stimulus inactivity. 4 recordings analyzed.

## 4 Conclusion

Synchronous network-wide bursting modulated stimulus/response relations. The duration of pre-stimulus inactivity critically determined response properties. We propose that activity-dependent synaptic depression shuts down excitability. Subsequent recovery entails shorter delays. Targeted interaction with ongoing activity confined response variability.

### Acknowledgement

We thank S. Kandler for valuable help in cell culturing and Patrick Pauli for technical assistance. This work was supported by the German BMBF (FKZ 01GQ0420 & FKZ 01GQ0830) and by the EC (NEURO, No. 12788).

### References

- [1] Arieli A., Sterkin A., Grinvald A., Aertsen A. (1996). Dynamics of ongoing activity: explanation of the large variability in evoked cortical responses. *Science*, 273, 1868-1871
- [2] Kisley M.A., Gerstein G.L. (1999). Trial-to-trial variability and state-dependent modulation of auditory-evoked responses in cortex. *J. Neurosci.*, 19, 10451-10460
- [3] Azouz R., Gray C.M., (1999). Cellular mechanisms contributing to response variability of cortical neurons in vivo. *J. Neurosci.*, 19, 2209-2223
- [4] Wagenaar D., DeMarse T.B., Potter S.M. (2005). MeaBench: A toolset for multi-electrode data acquisition and on-line analysis. *Proceedings of the 2nd International IEEE EMBS Conference on Neural Engineering*, 16-19 March 2005, 518-521.

# Mapping of neuronal oscillations in acute hippocampal slices at high spatial resolution with Multi-Transistor Arrays

Christian Stangl<sup>1</sup>, Peter Fromherz<sup>1\*</sup>

<sup>1</sup> Max Planck Institute for Biochemistry, Dept. of Membrane and Neurophysics, Martinsried / Munich

\* Corresponding author. E-mail address: fromherz@biochem.mpg.de

The analysis of the dynamic of neuronal oscillations in acute brain slices often rests on simultaneous extracellular recordings at different sites. Planar metal electrode arrays and voltage sensitive dyes were used to probe the CA3/CA1 region of hippocampal slices at a spatial resolution of 100  $\mu\text{m}$  (temporal: 2-5 kHz) and 22  $\mu\text{m}$  (200-500 Hz), respectively [1]. However, it is desirable to record 2D maps of field potentials at very high spatio-temporal resolution to localise generators of oscillatory activity and to study their synchronicity.

To address this issue we used silicon chips with transistor arrays. It has been shown that planar field-effect transistors (FET) are well suited for the recording of field potentials in acute slices [2]: We found that the FET recordings were identical to micropipette electrode signals. In spite of inactive cells caused by cutting processes the recorded signals were about 40% of their maximum within the slice. The acute brain slice could be displaced during experiments which allowed the probing of prolonged areas at the same slice.

For recording 2D maps of field potentials at high spatial resolution we used CMOS-fabricated silicon chips with Multi-Transistor Arrays (MTA) which provide 16384 sensors within 1x1 mm<sup>2</sup> (spacing: 7.8  $\mu\text{m}$ ; sampling rate: 6 kHz). After stimulation by tungsten electrode the pathways Mossy fibres–CA3 and Schaffer collaterals–CA1 could be mapped at high resolution which demonstrates the capability of this technique.

To resolve 2D maps of complex field oscillatory activity we recorded epileptiform signals at Mg(2+) -free medium. Sharp wave complexes and phase-locked fast ripples in CA3 could be monitored in space and time. Spectral analysis revealed a synchronous ripple oscillation with its source tightly to the pyramidal cell layer. In a second step Carbachol was applied to induce field oscillations in the gamma and theta range. Highly synchronised oscillatory patterns along cornu ammonis and near the dentate gyrus could be resolved by the MTA at high spatial resolution. Spectral analysis localised synchronous oscillation generators at the CA3 pyramidal cell layer but waves of activity at the activated CA1.

## References

- [1] Mann EO, Suckling JM, Hajos N, Greenfield SA, Paulsen O. (2005): Perisomatic feedback inhibition underlies cholinergically induced fast network oscillations in the rat hippocampus in vitro. *Neuron* 45,1, 105-117
- [2] Stangl C, Fromherz P. (2008): Neuronal field potential in acute hippocampus slice recorded with transistor and micropipette electrode. *European Journal of Neuroscience* 27, 958-964

# Spontaneous calcium transients in cultured cortical networks during development

Yuzo Takayama<sup>\*</sup>, Hiroyuki Moriguchi, Kiyoshi Kotani, Yasuhiko Jimbo

Graduate School of Frontier Sciences, University of Tokyo, Japan

<sup>\*</sup> Corresponding author. E-mail address: Yuzo\_Takayama@ipc.i.u-tokyo.ac.jp

Spontaneous activity plays important roles in the development of neuronal networks. Developmental changes in the spontaneous firing pattern of cultured neurons have been extensively studied by using the microelectrode array (MEA) recording system. However, little is known about the transition of spontaneous intracellular calcium dynamics and the relationship between calcium oscillations and electrical activity during development. In the present work, we carry out simultaneous recording of spontaneous electrical activity and intracellular calcium oscillations of rat cortical networks cultured on MEA.

## 1 Introduction

Spontaneous activity of immature neurons regulates the establishment of the basic morphology and the functions of neuronal networks through the activity-dependent synaptic plasticity [1]. To identify the roles of this activity-dependent synaptic plasticity in developing neuronal networks, spatio-temporal extracellular electrical recording of cultured neuronal networks with a microelectrode array (MEA) is an appropriate method because of its capability of spatio-temporal, non-invasive recording [2]. On the other hand, it is widely recognized that calcium ion flux through the calcium-selective ion channel or receptor is required for synaptic plasticity. Little is known, however, about the developmental changes in intracellular calcium oscillations and their relationship to electrical activity transitions in cortical networks. In the present study, we attempt to characterize the spontaneous calcium dynamics in neuronal populations during development and assess its relationship to electrical firing patterns.

## 2 Methods

Cortical tissues were obtained from 18-day-old Wistar rat embryo and were dissociated by trituration after digestion with 0.02% Papain solution in calcium and magnesium-free HBSS. The dissociated cells were plated on MEA substrates previously coated with poly-D-lysine and laminin.

The MEA substrates used in this experiment had 64 indium-tin-oxide (ITO) microelectrodes. Extracellular voltage signals obtained through each electrode were amplified 2000 fold with a 64-channel pre-amplifier and were stored on the hard disk of a personal computer. A sampling rate of 25 kHz per channel was used. Electrical recording was carried out simultaneously with calcium imaging in Ringer's solution.

Spontaneous intracellular calcium transients were visualized with the calcium indicator fluo-4. The cultures were incubated for 20 minutes with a culture medium containing 10  $\mu\text{g/ml}$  of fluo-4/AM, and the solution was replaced with Ringer's solution. Intracellular calcium transients in mechanically stimulated cells were also visualized. A glass micropipette (tip diameter, several  $\mu\text{m}$ ) and a hydraulic micromanipulator were used to stimulate the cells.

## 3 Results

In one week cultures, periodic synchronized bursting was observed and was followed by synchronized calcium transients. In three weeks cultures, synchronized calcium transients were rarely observed despite the presence of highly complicated synchronized activity (Fig. 1). Between these two states, in two weeks cultures, slow, radial propagation of calcium waves independent of electrical activity was observed (Fig. 2). Pharmacological treatments with the purinergic receptor antagonist suramin and gap junction blocker 18- $\beta$  glycyrrhethinic acid revealed that the spontaneous radial calcium waves were mediated by the astrocytic network, and suggest that the astrocytic calcium waves can influence the electrical firing patterns of networks by locally affecting neuronal signalling.

## References

- [1] L.C. Katz, C.J. Shatz. (1996) Synaptic activity and the construction of cortical circuits. *Science*, 274, 1133-1138.
- [2] Y. Jimbo, T. Tateno, H.P.C. Robinson. (1999) Simultaneous induction of pathway-specific potentiation and depression in networks of cortical neurons. *Biophys. J.*, 76, 670-678.

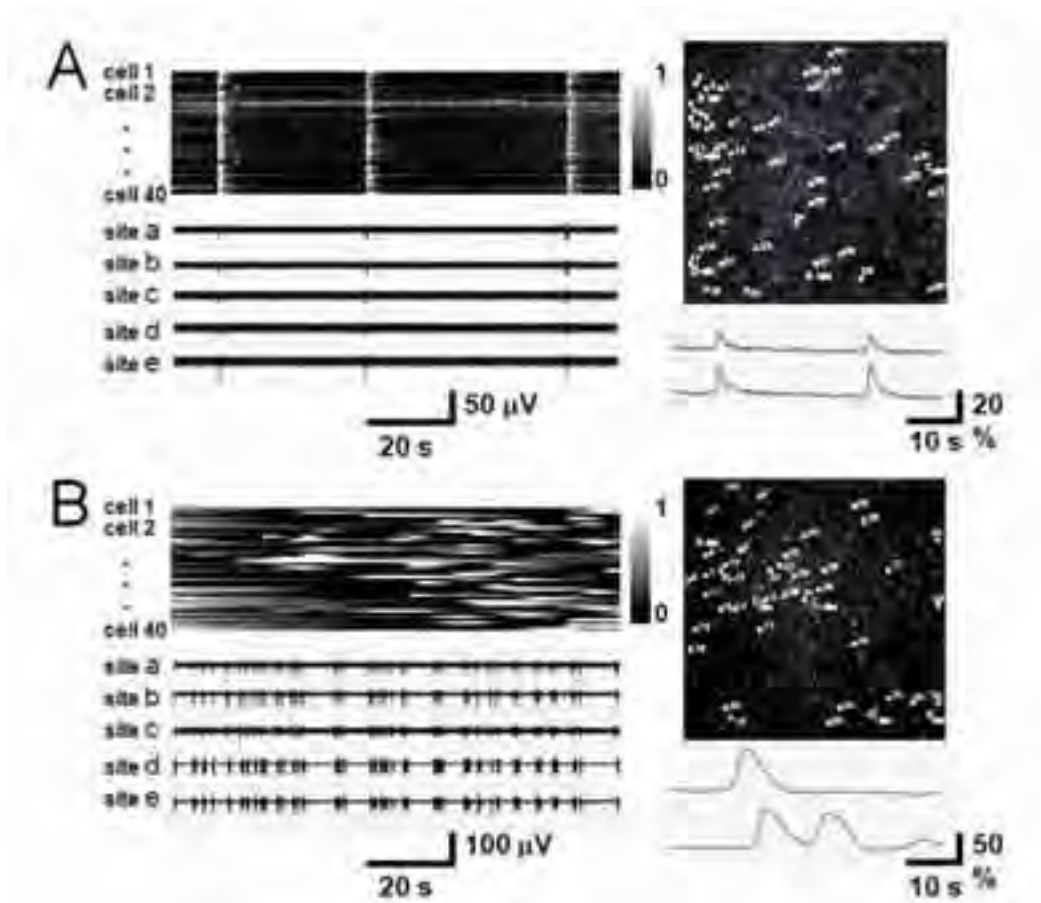


**Fig.1** Simultaneous recording of intracellular calcium transients and extracellular electrical signals. Electrical signals were obtained from five recording sites. Representative traces of calcium transients were also shown. *A*, Periodic synchronized bursting was followed by synchronized calcium transients in the immature stage ( $n=17$ ; at 8 DIV of this sample; 20 sec and 50  $\mu\text{V}$ ). *B*, Calcium transients were localized and did not follow non-periodic and complex synchronized bursting in the mature stage ( $n=10$ ; at 28 DIV of this sample; Scale bar, 20 sec and 100  $\mu\text{V}$ ).

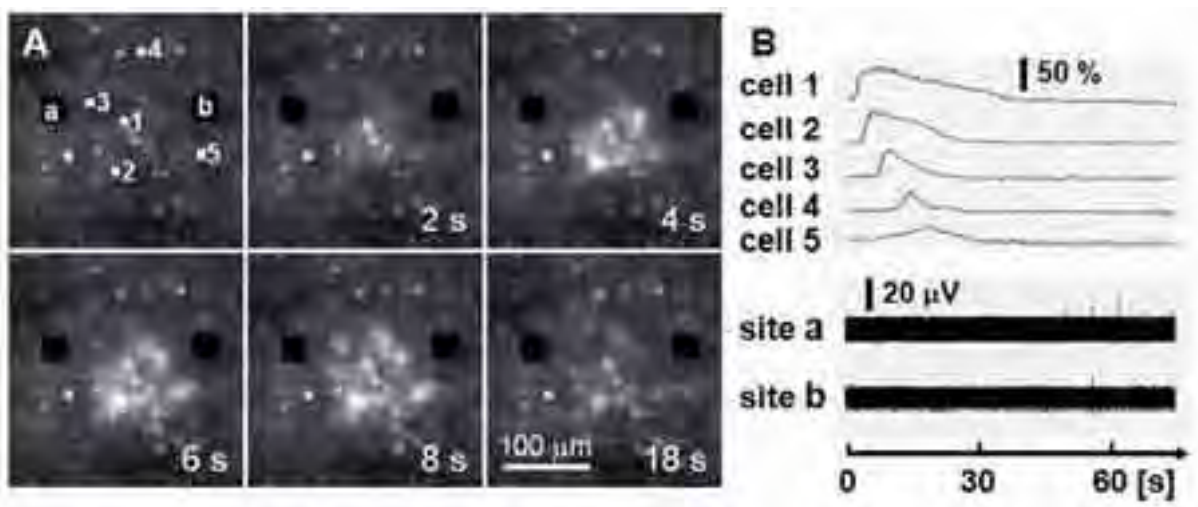


**Fig.2** Spontaneous calcium waves in a cultured cortical network. *A*, Spontaneous radial calcium waves were observed in the transition stage ( $n=13$ ; at 11 DIV of this sample.). *B*, Intracellular calcium transients and extracellular signals during spontaneous calcium waves. Traces of calcium transients and extracellular signals were obtained from five cells and two recording sites, respectively, indicated in (A).



# Self-wiring Neural Network Model for the Simulation of Connective Topology and Burst Propagation in Neuronal Cultures.

T. Gritsun<sup>\*</sup>, J. le Feber and W.L.C.Rutten

Neurotechnology group, Faculty of Electrical Engineering, Mathematics and Computer Science (EEMCS), University of Twente, Enschede, the Netherlands.

<sup>\*</sup> Corresponding author. E-mail address: t.gritsun@utwente.nl

Spiking activity has been studied to a great extent in network models with different topologies ranging from regular to random. Little is still known about activity of network models with more biologically plausible connective topology. In this research we analyze influence of more realistic topology rather than random on spatial patterns of spiking activity.

## 1 Introduction

State-of-the-art high-resolution MEAs enable to visualize in great detail the spatial propagation of bursting activity of cultured neuronal networks. Accordingly, in order to mimic the effect of burst propagation, modeling studies need to consider large scale neuronal networks (NNs) with plausible connective topology. Spiking activity has been studied to a great extent in network models with different topologies ranging from regular to random with different degree of randomness. Little is still known about simulated activity in models with biologically plausible connective topology. In this study we adopted several morphological models of the neurite growth to build a spatial connectivity map. This map is then used in simulations of spiking activity of large scale NNs that resemble bursting activity of neuronal cultures of dissociated cortical cells.

## 2 Methods

Van Pelt et al. (2003) used statistical findings of basic morphological features of cortical neurons to simulate neurite outgrowth [1]. To generate biologically plausible connective topology we used their model of neuronal morphogenesis in the NETMORPH simulation framework [2]. In addition we adopted chemotactic guidance model by [3] for the axonal guidance. Based on their methods we make connection strategies of the growing neuron in the 2D networks consisted of 10,000 to 50,000 neurons each generating thousands of synaptic connections with other neurons along outgrowing axons (see Fig. 1). Applied for all the neurons, this model creates a self-wiring network with connectivity maps that mimic realistic topology of neuronal cultures. At each simulation step of growing networks, generated connectivity maps entered the model of electrical activity.

To simulate spiking activity we used the same noise-driven network model as described in [4]. In brief the network was composed of Izhikevich neurons connected by frequency dependent synapses [5] to mimic short-term plasticity.

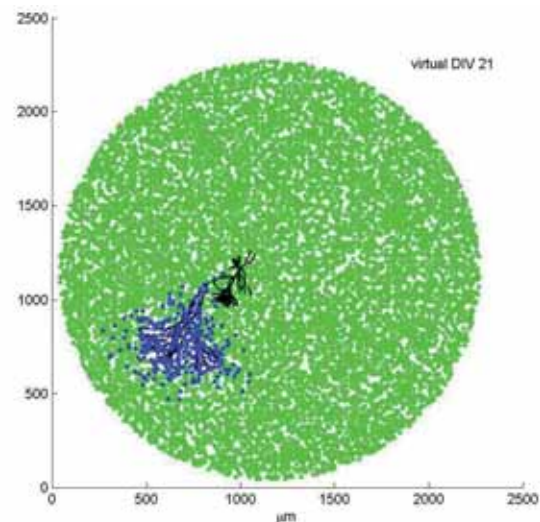


**Fig. 1.** A simulation of neurite tree (black line) growing in 2D network: a randomly selected pyramidal neuron. Cell somas are presented by dots: black for the mother soma for given axon, blue for the somas of the postsynaptic neurons connected to the selected mother soma and green for the rest.

## 3 Results

In our simulations NNs generated a big variety of network bursts (NBs) lasting from 100 to 500 ms. Bursts started spontaneously at random places or local areas which slowly recruited neighboring regions and propagated as waves through the whole NN. Figure 2 shows a 2D visualization of spiking activity acquired over 5 ms time window for each snapshot during NB. The layout of 60-electrode MEA was mapped onto the network topology map to pick up spiking activity around the virtual electrodes. To validate the data we calculated NB profiles as described in [6]. Figure 3

shows typical examples of spike raster and NB profiles acquired from the simulated network of 50,000 neurons. Simulated intra-burst features (e.g. NB profile shape) were similar to the experimental ones.

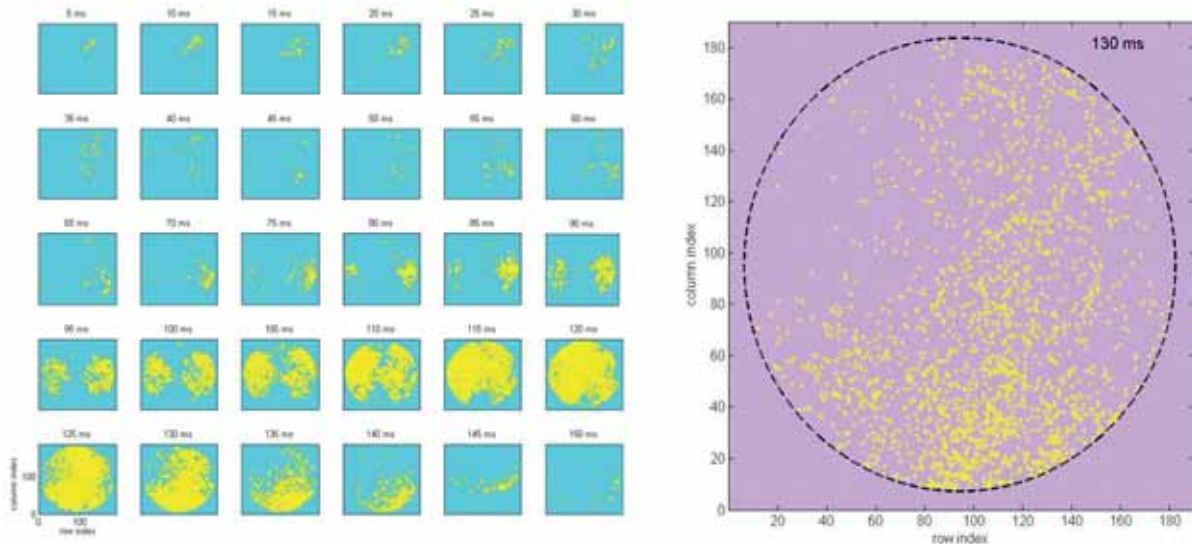


**Fig. 2.** An example of network burst presented as snapshot sequence on the left and enlarged snapshot at 130 ms on the right. Each snapshot shows spatial location of spikes (yellow dots) collected for 5 ms time window.

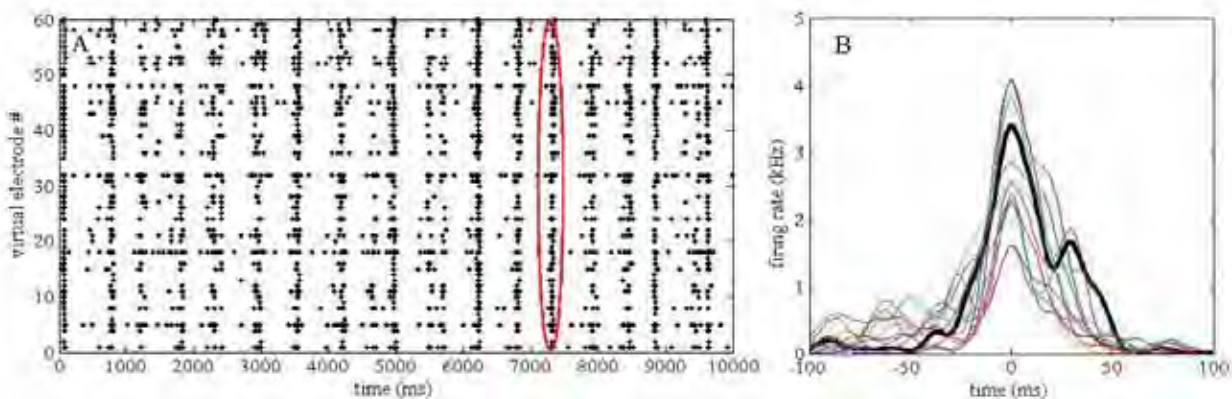


**Fig. 3.** Typical example of activity in large NN. A: activity around virtual electrodes; B: NB profiles calculated from the raster in A (red-marked burst in A shown in black in B).

## 4 Conclusions

Our results suggest that cortical neuronal cultures produce ‘wave-like’ propagation of synchronous NBs. This model can be used to closely examine spatial propagation of spiking activity patterns in cortical NNs.

### Acknowledgement

The work presented in this paper was funded by the EU Marie-Curie Neurovers-IT project (MRTN-CT-2005-019247).

### References

- [1] J. Van Pelt, and H.B.M. Uylings, Growth functions in dendritic outgrowth. *Brain and Mind* 4 (2003) 51-65.
- [2] R.A. Koene, B. Tijms, P. van Hees, F. Postma, A. de Ridder, G.J. Ramakers, J. van Pelt, and A. van Ooyen, NETMORPH: a framework for the stochastic generation of large scale neuronal networks with realistic neuron morphologies. *Neuroinformatics* 7 (2009) 195-210.
- [3] R. Segev, and E. Ben-Jacob, Generic modeling of chemotactic based self-wiring of neural networks. *Neural Networks* 13 (2000) 185-199.
- [4] T.A. Gritsun, J. Le Feber, J. Stegenga, and W.L.C. Rutten, Network bursts in cortical cultures are best simulated using pacemaker neurons and adaptive synapses. *Biological Cybernetics* 102 (2010) 1-18.
- [5] H. Markram, Y. Wang, and M. Tsodyks, Differential signaling via the same axon of neocortical pyramidal neurons. *Proceedings of the National Academy of Sciences of the United States of America* 95 (1998) 5323-5328.
- [6] J. Stegenga, J. le Feber, E. Marani, and W.L.C. Rutten, Analysis of cultured neuronal networks using intra-burst firing characteristics. *IEEE Trans Biomed Eng* (2008) 55 (4) 1382-1390.

# Simultaneous Recording of Synaptic Plasticity in CA1 and CA3 of APP.V717I Transgenic Mice Using Microelectrode Arrays

Seon-Ah Chong<sup>1,2</sup>, Carmen Bartic<sup>3,1</sup>, Wolfgang Eberle<sup>1</sup>, Fred Van Leuven<sup>4</sup>, Geert Callewaert<sup>2\*</sup>

<sup>1</sup> Bio-Electronic Systems, IMEC vzw, Leuven, Belgium

<sup>2</sup> Research Group Neurodegeneration, KULeuven, Kortrijk, Belgium

<sup>3</sup> Laboratory of Solid State Physics and Magnetism, Department of Physics and Astronomy, KULeuven, Leuven, Belgium

<sup>4</sup> Experimental Genetics Group LEGTEGG, KULeuven, Leuven, Belgium

\* Corresponding author. Geert.Callewaert@kuleuven-kortrijk.be

As an Alzheimer's Disease (AD) mouse model, APP.V717I transgenic mice show increased A $\beta$ 42 levels, cognitive impairment and amyloid plaques. To investigate early changes on synaptic dysfunction in this model, long term synaptic transmission in different hippocampal regions was monitored using microelectrode arrays. LTP was induced and recorded in CA3 and CA1 regions simultaneously in a same slice. We observed that LTP in CA3 was not altered at an early age although CA1 showed significant impairment in APP.V717I mice.

## 1 Background

Transgenic mice overexpressing mutant amyloid precursor protein APP.V717I have Alzheimer's Disease (AD)-like symptoms such as increased A $\beta$ 42 levels, cognitive impairment and amyloid plaques in the brain[1]. Already at early stages they show deficits in synaptic plasticity and deviating NMDA-receptor functions in the hippocampus[1;2]. Synaptic dysfunction studies in mouse models have been limited largely to recordings in CA1 region with conventional glass electrodes. Recent reports claimed that key molecules underlying A $\beta$  production affect synaptic plasticity in CA3 region[3;4]. Microelectrode array (MEA) enables us to record spatio-temporal patterns of biological signals as the most useful tool to measure the hippocampal circuits. In this study, we have used MEAs in order to monitor synaptic transmission changes in CA1 and CA3 regions simultaneously in APP.V717I transgenic mice as compared to wild-type mice.

## 2 Methods

### 2.1 Preparation of acute slices

APP.V717I transgenic mice were described previously[1]. Transgenic mice and littermates (age and sex matched) were anesthetized with CO<sub>2</sub> and decapitated. Hippocampal slices (250 $\mu$ m) obtained with a vibratome were kept in ice-cold ACSF solution containing (in mM) 125 NaCl, 2.5 KCl, 2 CaCl<sub>2</sub>, 1 MgCl<sub>2</sub>, 1.25 KH<sub>2</sub>PO<sub>4</sub>, 25 NaHCO<sub>3</sub> and 25 glucose. Slices were partially cut between CA3 and CA1 and allowed to recover in ACSF with constant oxygenation at least 2hr. Sections were placed onto 200/30 MEAs and perfused with oxygenated ACSF (2ml/min) at 31°C.

### 2.2 LTP induction and recording

LTP in CA3 and CA1 region was induced and recorded simultaneously in cut slices. Mossy fiber responses of CA3 were verified by frequency facilitation[5] before inducing LTP. Test stimuli were delivered every 60s and the amplitude was adjusted to 40% of the maximum field EPSP (fEPSP) response. LTP was induced by 2 trains of HFS (100Hz) with 20s interval.

### 2.3 Statistics

The standard error of mean values (mean  $\pm$  S.E.M.) was estimated and the data were compared by two sample *t*-test. Values of *P* < 0.05 were considered significant.

## 3 Results

To distinguish mossy fiber responses from associational-commissural (A/C) responses, we applied different stimulation frequencies and measured increased synaptic strength [6] in CA3 region. 4 month-old APP.V717I mice and littermates showed enhanced responses up to 150% to the stimulation (Fig. 1). Although the frequency facilitation in APP mice was slightly higher than the response in wild-type mice, it was not significantly different. Only electrodes showing frequency facilitation were chosen for LTP induction and recording in CA3. In addition, we cut slices between CA1 and CA3 to avoid the CA3 signals propagating to CA1 and to obtain separate LTP recording in the same slice. HFS-induced LTP lasted longer than an hour in both regions of the hippocampus. APP mice

showed significantly impaired long-term potentiation in CA1, on the other hand, synaptic plasticity in CA3 showed similar level in both types of mice (Fig. 2). Therefore the combined results indicate that postsynaptic, NMDA receptor-dependent LTP is impaired, while short-term synaptic plasticity and presynaptic NMDA receptor-independent LTP is normal in APP.V717I transgenic mice.

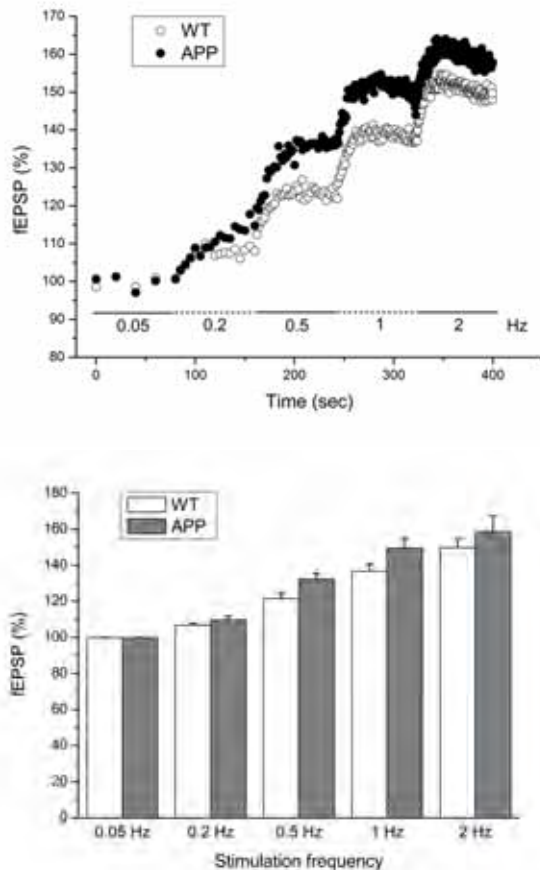


**Fig. 1.** Mossy fiber synapses in APP.V717I mice and littermates showed synaptic strength to increased stimulation frequencies (from 0.05Hz to 2Hz, upper panel). The frequency facilitation in both groups was not significantly different (lower panel).

#### 4 Conclusion/Summary

We have investigated synaptic transmission changes in different hippocampal regions in APP transgenic mice using a dual LTP recording technique. We observed that LTP in CA3 was not altered at an early age although CA1 showed significantly impaired LTP in APP.V717I mice.

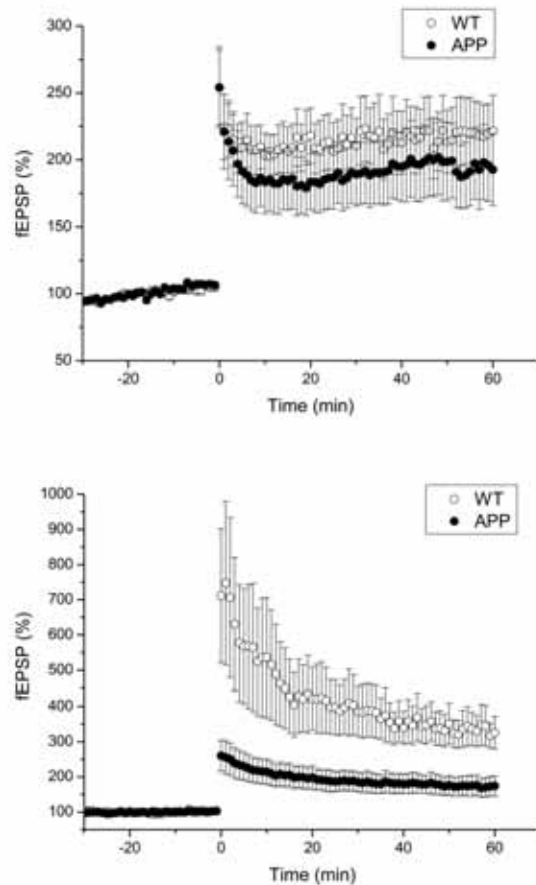


**Fig. 2.** After 30min of baseline recordings, 2 sets of HFS were applied to induce LTP. fEPSPs in CA3 were increased up to 180-200% and lasted for an hour. CA3 LTP of APP mice was similar to that of wild types (upper panel). On the other hand, APP.V717I mice showed significant decrease of LTP in CA1 (lower panel).

#### References

- [1] Moechars, D., Dewachter, I., Lorent, K., Reverse, D., Baekelandt, V., Naidu, A., Tesseur, I., Spittaels, K., Van Den Haute, C., Checler, F., Godaux, E., Cordell, B., and Van Leuven, F. (1999) *Journal of Biological Chemistry* 274, 6483-6492
- [2] Dewachter, I., Filipkowski, R. K., Priller, C., Ris, L., Neyton, J., Croes, S., Terwel, D., Gysmans, M., Devijver, H., Borghgraef, P., Godaux, E., Kaczmarek, L., Herms, J., and Van Leuven, F. (2009) *Neurobiology of Aging* 30, 241-256
- [3] Wang, H., Song, L., Laird, F., Wong, P. C., and Lee, H. K. (2008) *Journal of Neuroscience* 28, 8677-8681
- [4] Zhang, C., Wu, B., Beglopoulos, V., Wines-Samuels, M., Zhang, D. W., Dragatsis, I., Sudhof, T. C., and Shen, J. (2009) *Nature* 460, 632-U100
- [5] Nicoll, R. A. and Schmitz, D. (2005) *Nature Reviews Neuroscience* 6, 863-876
- [6] Salin, P. A., Scanziani, M., Malenka, R. C., and Nicoll, R. A. (1996) *Proceedings of the National Academy of Sciences of the United States of America* 93, 13304-13309

# Consequences of excessive 5-HT levels during development on signal propagation and short term plasticity in the rat barrel cortex in vitro

Dirk Schubert<sup>\*</sup>, Martijn Selten, Thomas Slippens, Judith Homberg, Rembrandt Bakker, Rolf Kötter

Donders Institute for Brain, Cognition and Behaviour, Department of Cognitive Neuroscience, Radboud University Medical Centre, Nijmegen, The Netherlands

<sup>\*</sup> Corresponding author. E-mail address: d.schubert@donders.ru.nl

In rodents increased 5-HT levels during brain development leads to structural changes in the lemniscal thalamocortical pathway of the somatosensory system. In the present study we investigated whether and to which extent a genetically knock out of the 5-HT transporter (5-HTT KO) in rats affects the functional connectivity in the primary somatosensory cortex. By employing multi-electrode-array (MEA) recordings of local field potentials (LFPs) on acute thalamocortical slice preparations we could show that compared to wildtype animals, 5-HTT KO rats display higher short time plasticity, especially for LFPs being induced in the supragranular layers. This indicates that in addition to afferent thalamocortical pathways also intracortical networks are being changed by excessive 5-HT levels during brain development.

## 1 Introduction

Selective serotonin transporter (5-HTT) inhibitors (SSRIs) are commonly-used antidepressants during pregnancy, which leads to high serotonin levels in the foetus (for review see [1]). In rodents a dysfunction of 5-HT transporters during brain development causes distorted wiring in afferent pathways of sensory systems, such as the lemniscal thalamocortical pathway between the ventral posteromedial thalamic nucleus (VPM) and the primary somatosensory (barrel) cortex. These structural changes in the afferent pathway might have profound effects on structure and function within the barrel cortex, too. Here we investigated how synaptic signal propagation and short-term plasticity are affected in the well-defined cortical microcircuits of the rat barrel cortex when 5-HTT expression has been genetically knocked out.

## 2 Material & Methods

We employed extracellular multi-electrode-array (MEA) recordings of local field potentials (LFPs) on acute thalamocortical brain slice preparations of juvenile (P21-23) wildtype and 5-HTT knock out (5-HTT KO) rats. We tested signal propagation and short term plasticity of layer and column specific synaptic responses by application of paired-pulse electrical stimulation (interstimulus interval 50 ms) in cortical layers II to VI [2]. In both animal models signals were induced under physiological conditions as well as following long time exposure to 5-HT (10  $\mu$ M). Analysis was performed on LFP and 2-dimensional current source density data.

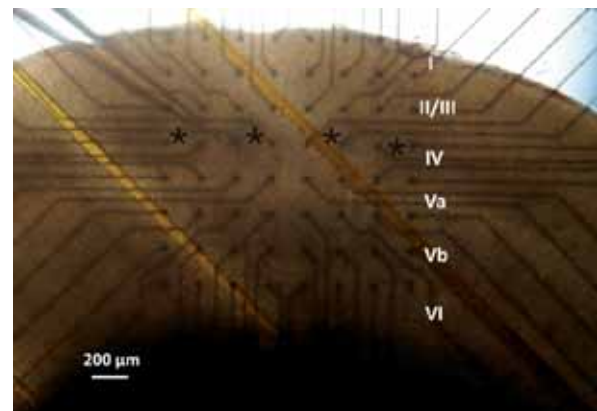


**Fig. 1.** Acute thalamocortical brain slice preparation of the primary somatosensory cortex mounted on top of a 60 TiN electrode MEA in an upright microscope setting under low magnification (10x). Asterisks mark the positions of barrels in layer IV.

## 3 Results

In 5-HTT KO rats the spatial extent of signal propagation following stimulation of layers II to VI was similar to that in wildtype rats. Furthermore, under physiological conditions stimulation of infragranular layers Va, Vb and VI resulted in no significant differences between LFP response properties of 5-HTT KO and wildtype rats. However LFP responses involving the intracolumnar layer IV to layers II/III pathway showed significant alterations in 5-HTT KO rats. LFPs in layers II/III showed decreased initial response amplitudes and increased short term facilitation after stimulating intracolumnarly in layer IV as well as in layer II/III.

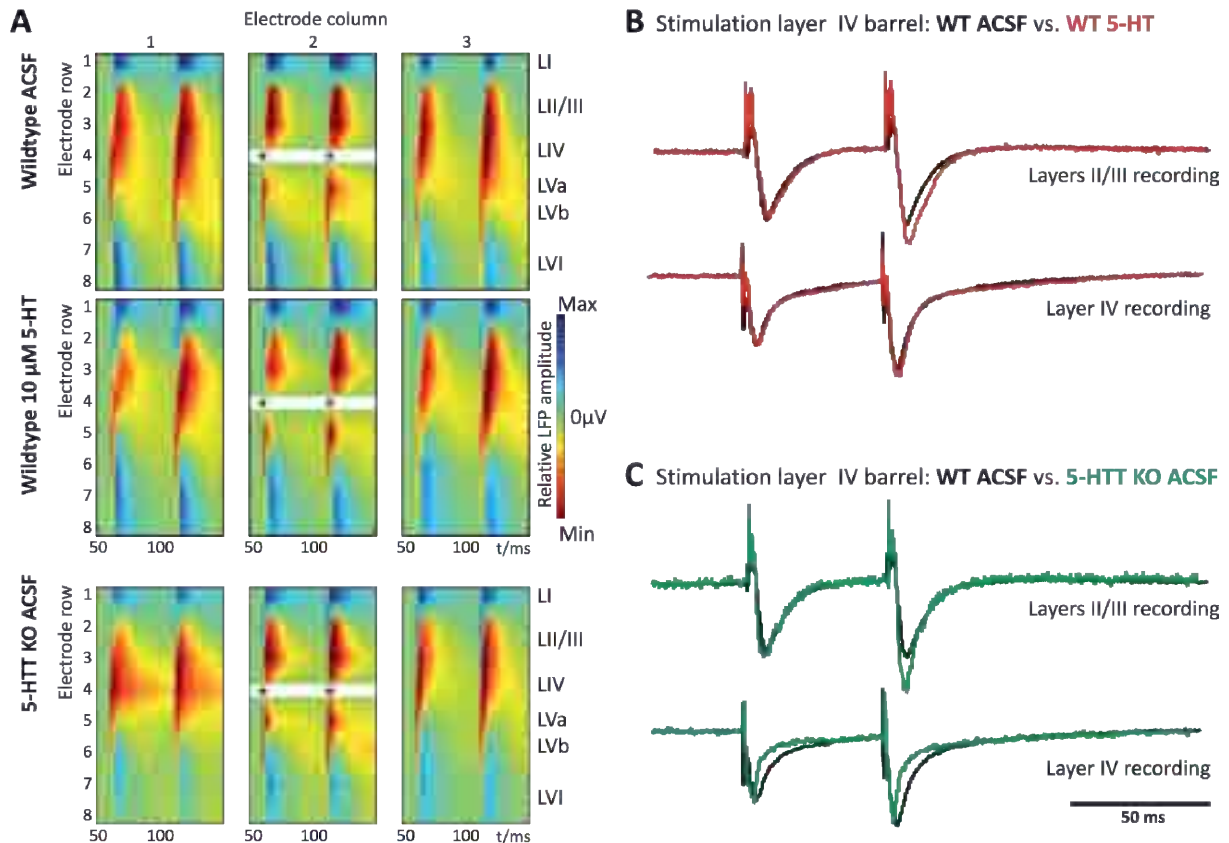


**Fig. 2.** LFP responses following paired pulse stimulation in layer IV. A) Propagation of LFP responses (normalized amplitudes) in wildtype (WT) and 5-HTT KO animals, given for three adjacent electrode columns each. The asterisks mark location and timing of the electrical stimulation in layer IV. B) Sample traces of LFP responses taken from the same electrodes in layers II/III and layer IV averaged over 8 sweeps. Following layer IV stimulation under 5-HT application paired pulse facilitation (PPF) is increased in layers II/III whereas PPF remains unchanged in layer IV. C) Sample traces of LFP responses taken from similar recording positions in layer II/III and layer IV. Under physiological conditions 5-HTT KO rats display increased PPF in layers II/III whereas in layer IV PPF is similar to that of the wildtype animals. For reasons of simplification LFP amplitudes have been normalized.

These changes were detected not only in supragranular responses of the home-column but also in those of the neighbouring column. A similar layer-specific alteration of LFP plasticity could be induced by long term applications of 10  $\mu\text{M}$  5-HT in wildtype brain slices. In 5-HTT KO rats, however, long term application of 5-HT had no significant effect on layers II/III responses.

## 4 Conclusions

Our data indicate that increased 5-HT levels during brain development do not only affect the wiring in the afferent pathways of the rodent somatosensory system (e.g. thalamocortical afferences, Homberg et al., 2010) but also the intracortical networks. We found evidence of changes that involve the intracortical pathway which transmits sensory information from the main target layer for thalamocortical afferences of the lemniscal pathway, granular layer IV, to the associative layers II/III. Altered synaptic responses and plasticity in these layers might eventually contribute to changed tactile sensation and behaviour.

## References

- [1] J.R. Homberg†, D. Schubert†, P. Gaspar: New perspectives on the neurodevelopmental effects of SSRIs; *Trends Pharmacol. Sci.*, 2010 (31): 60-65
- [2] R. Bakker, D. Schubert, K. Levels, G. Bezgin, I. Bojak, R. Kötter: Classification of Cortical Microcircuits based on Micro-Electrode-Array Data from Slices of Rat Barrel Cortex, *Neural Networks* 2009, 22: 1159-1168.

# Network hyperexcitability of cortical cultures from synapsin I knockout mice grown onto Micro-Electrode Arrays

Michela Chiappalone<sup>1\*</sup>, Valentina Pasquale<sup>1</sup>, Mariateresa Tedesco<sup>2</sup>, Sergio Martinoia<sup>1,2</sup> and Fabio Benfenati<sup>1,3</sup>

<sup>1</sup> Department of Neuroscience and Brain Technology, Italian Institute of Technology, Genova (Italy)

<sup>2</sup> Department of Biophysical and Electronic Engineering, University of Genova, Genova (Italy)

<sup>3</sup> Department of Experimental Medicine, Section of Physiology, University of Genova, Genova (Italy)

\* Corresponding author. E-mail address: michela.chiappalone@iit.it

Synapsins are synaptic vesicle phosphoproteins that play a role in synaptic transmission and plasticity by acting at multiple steps of exocytosis. Mutation of *SYN1* gene results in an epileptic phenotype in mouse and man, implicating SynI in the control of network excitability. In this study we analyzed the excitability and network dynamics of primary cortical neurons from wild-type (WT) and SynI knockout (SynIKO) mice grown onto Micro-Electrode Arrays (MEAs). The use of MEAs allowed us to record the electrophysiological activity of cortical cultures at different ages during development (up to 35 days in vitro) and under the effect of pharmacological and electrical stimulation. The Self Organized Criticality (SOC) theory was applied to study the neuronal avalanche phenomenon in both genotypes.

## 1 Introduction

Epilepsy syndromes have a large genetic component. Although a large number of genes have been inactivated in animal models, only few mutants exhibit an epileptic phenotype, namely knockout (KO) mice lacking members of the synapsin (Syn). Synapsins (Syns) are synaptic vesicle phosphoproteins that play a role in synaptic transmission and plasticity by acting at a multiple steps of exocytosis. Recently, a form of familial epilepsy characterized by a non-sense mutation in the *SYN1* gene that was present in all affected family members was reported [1].

In this study we performed experiments on cortical networks from KO and WT (i.e. wild type) embryonic mice grown on Micro-Electrode Arrays, in order to characterize the intrinsic dynamics of such preparations and to unveil the origin of hyperexcitability which characterizes KO networks.

## 2 Materials and Methods

SynI KO mice were generated by homologous recombination. Cortical neurons extracted from embryos (E17) of both WT and KO mice were cultured on planar arrays of 60 TiN/SiN electrodes (Multi Channel Systems® - MCS, Reutlingen, Germany), pre-treated with adhesion factors (Poli-L/D-Lysine and Laminin).

Extracellular signals recorded by MEAs are characterized by the presence of two distinct patterns of activity: spikes and burst. Spikes are identified by a threshold-based algorithm [2], while bursts are recognized by an innovative self-adapting algorithm [3]. Cross-correlation is applied to the burst event

point process [4], in order to assess the synchronization level among all recording sites.

### 2.1 Experimental protocols

For developmental studies, the spontaneous activity was monitored and recorded for 20-30 minutes at various ages, namely at 12-15, 18-20, 24-26 and 31-35 DIV. Pharmacological studies were performed on 24-35 DIV cultures. Spontaneous activity in physiological solution was recorded for 20 min (control condition). Then, networks were exposed to the GABA<sub>A</sub> receptor antagonist bicuculline (BIC, Tocris, Bristol, UK) added at the final concentration of 30  $\mu$ M [5] and the recording session continued for additional 20 min.

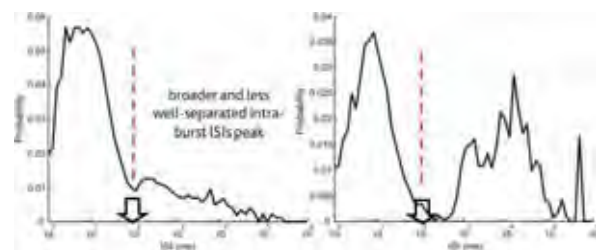


**Fig. 1.** Network ISI histogram obtained for a KO (left) and a WT (right) culture

## 3 Results

To study the cellular bases of the high susceptibility to epileptic seizures of mice lacking SynI, we first analyzed the spontaneous electrical activity of networks of cortical E17 primary neurons prepared from WT and SynI KO embryos and plated onto MEAs.

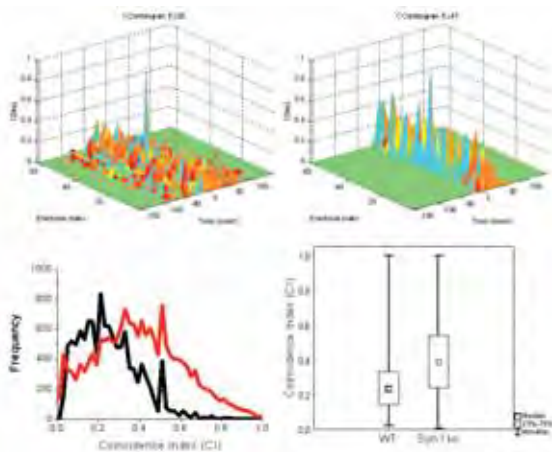


**Fig. 2.** The cross-correlograms of the bursting activity recorded by one channel versus all the others in a WT (left) and one SynIKO (right) culture.

The spontaneous activity of the cultures from both genotypes is characterized by a balanced presence of random spikes and bursts, but SynI KO networks display a much higher spiking and bursting activity than WT networks. More specifically, bursting behavior in SynIKO cultures is organized in long sequences of closely packed network bursts (*superbursts*), instead of well-separated barrages, as more often displayed by WT cultures (Fig. 1).

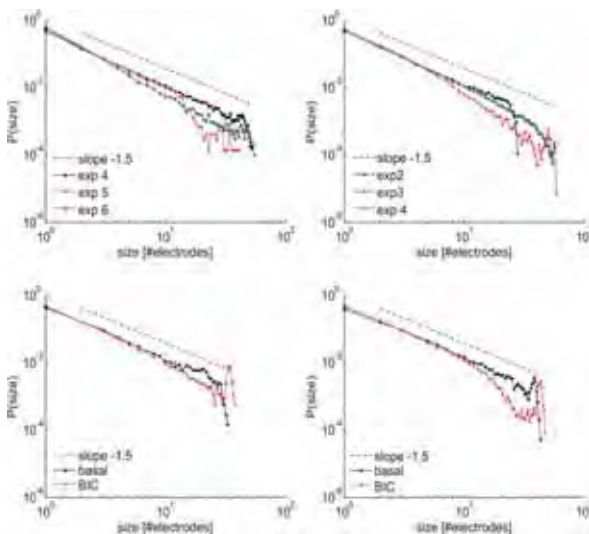


**Fig. 3.** Avalanche size distribution for WT (left) and SynIKO (right) cultures during spontaneous (top) and BIC-induced (bottom) activity.

The cross-correlograms (Fig. 2) of the bursting activity recorded by all the possible pairs of electrodes (59x59, excluding autocorrelation) show that, under basal conditions, the SynI KO preparation presents a higher number of synchronized channels. In addition, the level of synchronization reaches its maximum values in most of the bursting channels and the correlation peak is much sharper. The histograms for CI (Coincidence Index) further confirm a higher level of synchronization for the KO networks.

Preliminary results (Fig. 3), obtained in the light of the SOC theory, show that during spontaneous activity WT cultures exhibit subcritical behavior more often than critical or supercritical; whereas SynIKO cultures tend to critical and supercritical states. The addition of BIC (30  $\mu$ M) induces a transition from criticality to supercriticality in both genotypes.

## 4 Conclusions

Our results demonstrate that the ablation of the SYN1 gene is associated with a highly increased spontaneous activity, with more frequent and sustained bursts and a higher degree of synchronization in the network. Preliminary results, obtained in the light of the SOC theory demonstrate that SynIKO cultures during spontaneous activity generally tend to a critical/super-critical state. These results can provide further explanation for the high susceptibility of SynIKO mice to epileptic seizures.

## Acknowledgement

The project was supported by grants from the Ministry of the University and Research Grants (PRIN 2006) and Compagnia di San Paolo. We thank drs. Paul Greengard (The Rockefeller University, New York, NY) and Hung-Teh Kao (Brown University, Providence, RI) for providing us with the mutant mouse strains and for invaluable discussions.

## References

- [1] Garcia C. C., Blair H. J., Seager M., Coulthard A., Tennant S., Buddles M., Curtis A. and Goodship J. A. (2004). Identification of a mutation in synapsin I, a synaptic vesicle protein, in a family with epilepsy *Journal of Medical Genetics*, 41, 183-186.
- [2] Maccione A., Gandolfo M., Massobrio P., Novellino A., Chiappalone M. and Martinoia S. (2009). A novel spike detection algorithm for real time applications. *Journal of Neuroscience Methods*, 177,1, 241-249.
- [3] Pasquale V., Martinoia S. and Chiappalone M. (2009). A self-adapting approach for the detection of bursts and network bursts in neuronal cultures. *Journal of Computational Neuroscience*,
- [4] Chiappalone M., Vato A., Berdondini L., Koudelka-Hep M. and Martinoia S. (2007). Network dynamics and synchronous activity in cultured cortical neurons. *International Journal of Neural Systems*, 17,2, 87-103.
- [5] Keefer E. W., Gramowski A. and Gross G. W. (2001). NMDA receptor-dependent periodic oscillations in cultured spinal cord networks. *Journal of Neurophysiology*, 86, 3030-3042.



# Persistent effects of cholinergic activation in developing cerebral cortex cultures: a model for the role of sleep activity patterns in early development?

Chiappalone Michela<sup>1</sup>, Corner Michael<sup>2\*</sup>, Le Feber Joost<sup>3</sup>

<sup>1</sup> Department of Neuroscience and Brain Technologies, Italian Institute of Technology, Genova (Italy)

<sup>2</sup> Systems Biology Laboratory, Israel Institute for Technology - Technion, Haifa (Israel)

<sup>3</sup> MIRA Institute for Biomedical Engineering and Technical Medicine, University of Twente, Enschede (The Netherlands)

\* Corresponding author. E-mail address: m.corner@hccnet.nl

The effects of prolonged (overnight) cholinergic activation, by means of continuous exposure to carbachol, were studied in 3-week-old rat neocortical networks cultured on a 60-electrode Micro-Electrode Array (MEA). Carbachol consistently produced a persistent strong change in spontaneous neuronal firing which mimics ‘desynchronized’ firing patterns characteristic of REM sleep in situ. Upon return to control medium, activity quickly returned to the original quasi-(slow wave) sleep pattern, but at an enhanced level of synchronized bursting which could persist for at least 24 hours.

## 1 Introduction

Spontaneous spiking activity in the sleeping neocortex typically takes the form of synchronous poly-neuronal bursts which are now known to homeostatically regulate network excitability (for a recent comprehensive review, [1]). The questions now arise of (1) does the hyperactivity which typically results from prolonged suppression of these bursts extend to the ‘desynchronized’ cholinergically activated state? and (2) does prolonged, REM sleep-like, cortical ‘arousal’ in turn affect spontaneous synchronous bursting patterns upon return to control conditions?

## 2 Materials and Methods

Cell cultures prepared from neonatal rats were cultured for 3 weeks in vitro on multi-electrode arrays and, after being monitored for a few hours in the growth medium, were exposed to carbachol (20  $\mu$ M) for ca. 20h, following which they were returned to control medium for another 20 some odd hours of recording. A second group was treated similarly after pre-treatment with tetrodotoxin (TTX, 1 $\mu$ M) for ca. 20h.

Activity patterns were analysed by observation of raster plots and by calculating burst rates, inverse burst ratios [2] (i.e. percentage of spikes outside the bursts), autocorrelations and functional connectivity [3].

All acquisitions were identical to the protocols reported for previous studies from the Marom lab, simultaneously recording signals from 60 electrodes at a sample frequency of 24 kHz [4].

## 3 Results

All pre-carbachol recordings showed a persistent pattern of recurring brief (50-100ms) bursts which were tightly synchronized across all active electrodes. This pattern was consistently associated with high functional connection strengths, reflecting high intensity of excitatory synaptic interactions within the network.

Network bursts tended to be more frequent in the TTX pre-treated cultures, along with an overall enhancement of network firing rates (cf. Figs. 1 & 2). Somewhat surprisingly, the TTX group also showed a lower percentage of spikes within bursts (‘burst ratio’) and, consequently, higher inter-burst firing rates.

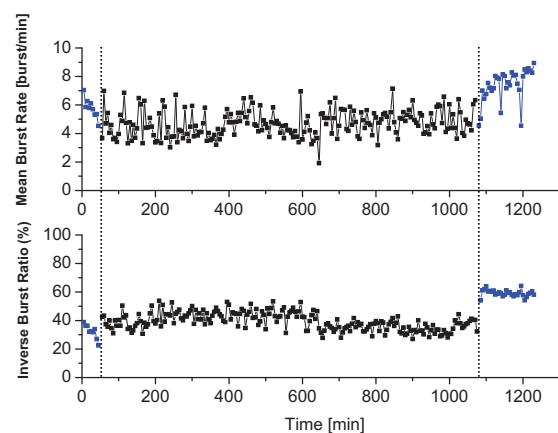
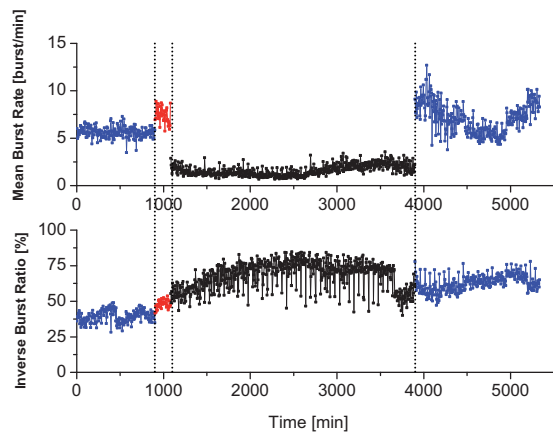


Fig. 1. Mean Bursting Rate (top) and Inverse Burst Ratio (percentage of spikes outside the burst, bottom) for a control culture. Experiment sequence: neurobasal medium (blue line) – carbachol 20 $\mu$ M (black line) – neurobasal medium (blue line).

Firing levels within bursts (burst ‘intensity’) were not noticeably affected, however, nor were the mean durations of the bursts.

Upon transfer to a carbachol-containing medium (20  $\mu\text{M}$ ), 'phasic' network activity in all cases became visibly much more variable and less tightly synchronized, while trains of largely uncorrelated firing appeared on various channels. Burst ratio and intensity levels decreased whereas interburst firing rates increased, all to a greater extent in the TTX pre-treated group than in the controls (Fig. 1, 2). These observations were confirmed by inspection of raster plots and calculation of a 'burstiness index' as described in [5]. The autocorrelation and the array wide mean firing rate declined considerably in all cases. Particularly, the mean firing rate decrease in the TTX experiments was larger than control. As in the controls, after 5-6 hours bursts tended to become visibly more synchronized again and to move slowly towards the pre-carbachol parameter values. Autocorrelations and mean firing rates nevertheless remained steady at the reduced levels for the rest of the treatment.



**Fig. 2.** Mean Bursting Rate (top) and Inverse Burst Ratio (percentage of spikes outside the burst, bottom) for a TTX-pre-treated culture. Experiment sequence: neurobasal medium (blue line) - TTX 1  $\mu\text{M}$  (24 hours long, not reported) - wash out after pre-treatment with 1  $\mu\text{M}$  TTX (red line) - carbachol 20  $\mu\text{M}$  (black line) - neurobasal medium (blue line).

Upon return to control medium after carbachol treatment, firing patterns in all cases showed a reappearance of highly synchronized firing, as confirmed by a re-increase of autocorrelations, which then remained largely unchanged for at least 20h. Mean firing and burst rates, as well as interburst firing rates, were augmented above their original levels in the control group, to the extent that they approximated the values seen immediately following TTX treatment. Burst ratios were also lower now, and here too attained a similar level as in the TTX group prior to exposure to carbachol (fig. 1, 2). Indeed, the sole parameter distinguishing between the effects of prolonged carbachol versus acute TTX treatment was the intra-burst spiking intensity, which was considerably higher in the latter group. Post-carbachol firing in TTX pre-treated cultures, in contrast, was characterized by an exceptionally high incidence of synchronized bursts, high interburst firing levels and

long-lasting burst durations in comparison with post-carbachol values in control cultures (fig. 1, 2).

## 4 Conclusions

In view of the striking similarity between the effects of carbachol and TTX treatments, the importance of REM sleep (pure extrinsic cholinergic activation) for cortical maturation may not be, after all, to provide needed stimulation but, on the contrary, to permit intrinsic excitatory growth mechanisms and interconnections to mature without being counteracted by opposite effects mediated via synchronous polyn neuronal burst discharges such as occur during slow-wave sleep.

## Acknowledgement

Acquisition of the reported data was made possible by the kind hospitality of Profs. M. Marom and N. Ziv during M. Corner's stay in their lab in March/April, 2009.

## References

- [1] Corner M. A. (2008). Spontaneous neuronal burst discharges as dependent and independent variables in the maturation of cerebral cortex tissue cultured in vitro: a review of activity-dependent studies in live 'model' systems for the development of intrinsically generated bioelectric slow-wave patterns. *Brain Res Rev*, 59,1, 221-244.
- [2] Chiappalone M., Bove M., Vato A., Tedesco M. and Martinoia S. (2006). Dissociated cortical networks show spontaneously correlated activity patterns during in vitro development. *Brain Res*, 1093,1, 41-53.
- [3] le Feber J., Rutten W. L. C., Stegenga J., Wolters P. S., Ramakers G. J. A. and van Pelt J. (2007). Conditional firing probabilities in cultured neuronal networks: a stable underlying structure in widely varying spontaneous activity patterns. *J Neural Eng*, 4, 54-67.
- [4] Eytan D. and Marom S. (2006). Dynamics and effective topology underlying synchronization in networks of cortical neurons. *J Neurosci*, 26,33, 8465-8476.
- [5] Wagenaar D. A., Madhavan R., Pine J. and Potter S. M. (2005). Controlling bursting in cortical cultures with closed-loop multi-electrode stimulation. *J Neurosci*, 25,3, 680-8.

# Burst- induced Inhibition in Cortical Neuronal Networks *in vitro*

Tom Reimer<sup>1</sup>, Werner Baumann<sup>1</sup>, Philipp Julian Koester<sup>1</sup>, Jan Gimsa<sup>1\*</sup>

<sup>1</sup> University of Rostock, Chair for Biophysics, Gertrudenstrasse 11a, 18057 Rostock, Germany

\* E-mail address: jan.gimsa@uni-rostock.de

We analyzed the interactions in the electric activity of different neuron types in low density cortical networks growing on MEA glass neurochips. During spontaneous activity, irregularly spiking neurons (theta-beta oscillators) were curbed by simultaneously bursting neurons (gamma oscillators). This kind of interaction might be an important principle in the restriction of excitation and the processing of information in the cerebral cortex.

## 1 Background

The mechanisms balancing excitation and inhibition as well as restricting and stabilizing excitation in the cerebral cortex are still not well understood. A detailed analysis is hindered by the complex, dense structure of the native cortex. Cortical neuronal networks growing on MEAs allow for a simplification and an easier modelling of the cortical “Faserfilz” [1]. The networks show complex, nonlinear firing patterns in their spontaneous activity. This self-organized activity is ubiquitous in all mammalian brains and understanding it is one of the most important challenges in neuroscience. Different patterns of neuronal avalanches as well as single-neuron activity may coexist in the same network because of the diversity of cortical neurons. Our research aims at clarifying how the different neurons or neuronal groups act and interact in concert.

## 2 Methods

Cortices were carefully prepared from embryonic mice (E15) followed by enzymatic dissociation. Cells were plated at densities of 1000 – 3000 cells/mm<sup>2</sup> on poly-D-lysine/laminin coated miniaturized glass neurochips (16 x 16 mm<sup>2</sup>, developed at the Chair for Biophysics, University of Rostock) with integrated 52-microelectrode arrays (MEA) [2]. The culture area was 20 mm<sup>2</sup>. Cultures were incubated at 10 % CO<sub>2</sub> and 37 °C for four weeks. Half of the medium was replaced thrice a week. Recordings were performed with our modular glass chip system (MOGS) coupled to a preamplifier and data acquisition software (Plexon Inc., Dallas, TX, USA). For morphological characterization, networks were fixed with paraformaldehyd and immunohistochemically stained against parvalbumin and neurofilament 200 kD before confocal laser scanning microscopy.

## 3 Results

Nearly all low density networks exhibited at least two different firing patterns in their spontaneous activity. Different forms of oscillations co-existed in the networks. We found simultaneously bursting neurons (gamma oscillators, accounting for the majority of the detected units) curbing irregularly spiking neurons (theta-beta oscillators, accounted for the minority of detected units) in many networks. In the literature, bursting neurons were often identified as excitatory pyramidal cells. Our preliminary data suggest that the bursting neurons are parvalbumin-expressing interneurons with abundant axonal ramifications. These neurons show parvalbumin-localization especially in the cell soma and in their basal, partially distal dendrites. The strong axonal ramification could be the reason that the electric activity of these cells is detected by the MEA with a much higher probability. This would result in a biased detection in favour of interneuron-types, i.e. a disproportionally high number of detected units, even though they only account for a minority of neurons present in our networks.

## 4 Summary

The cultivation of small, low density cortical networks on MEAs is a reductionistic approach. It enables us to investigate self-organized neuronal networks with a structure much more simplified than the native cortex. As in the native cortex, these networks exhibit different activity patterns during autonomous spontaneous activity according to their cellular composition. Firing patterns of different neurons are usually not differentiated in mature networks. In contrast, our networks show complex, nonlinear patterns that imply interactions between different neurons and neuronal groups. In our *in vitro* system, the balance between excitation and inhibition is caused by the interaction of simultaneously bursting interneurons and irregularly spiking neurons. This

kind of interaction may play an important role in the processing of information in the cerebral cortex.

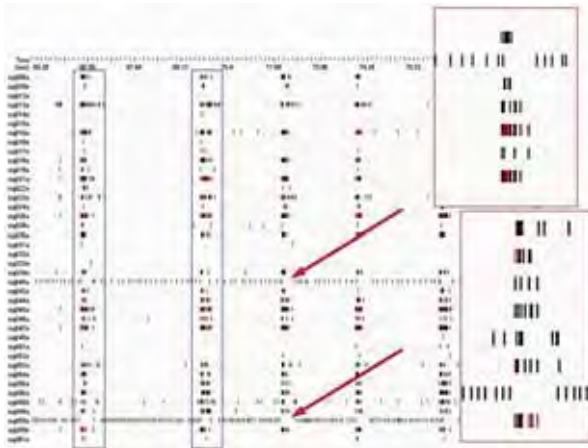


**Fig. 1.** Burst – induced inhibition. Simultaneously bursting neurons (blue boxes); curbed spiking neurons (red arrows). Red boxes: zooms of the arrow-marked areas. neurons inhibit the activity of the spiking neuron.

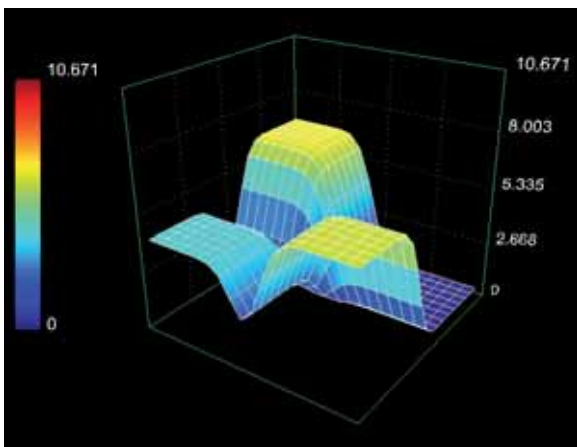
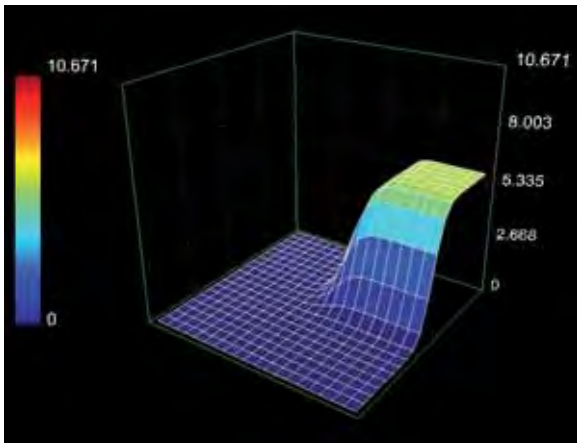


**Fig.1.1.**Activities of four neurons (units) selected from a network showing 40 units. Top: the 3 o'clock quadrant neuron is spiking during the silence of three bursting neurons (other three quadrants). Bottom: neighbouring bursting neurons inhibit the activity of the spiking neuron.

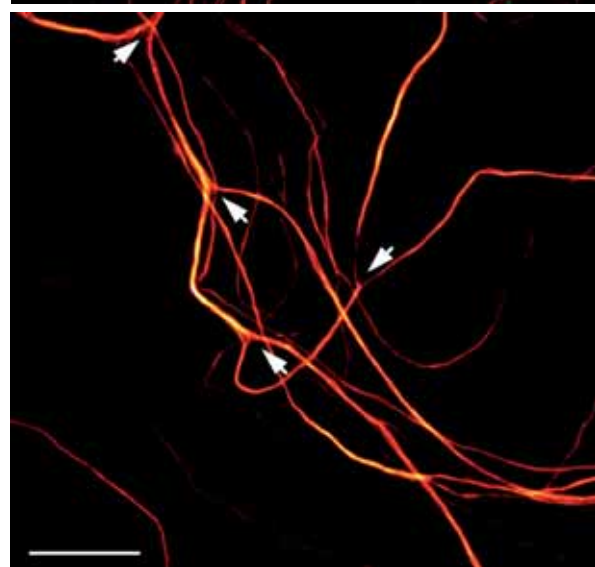
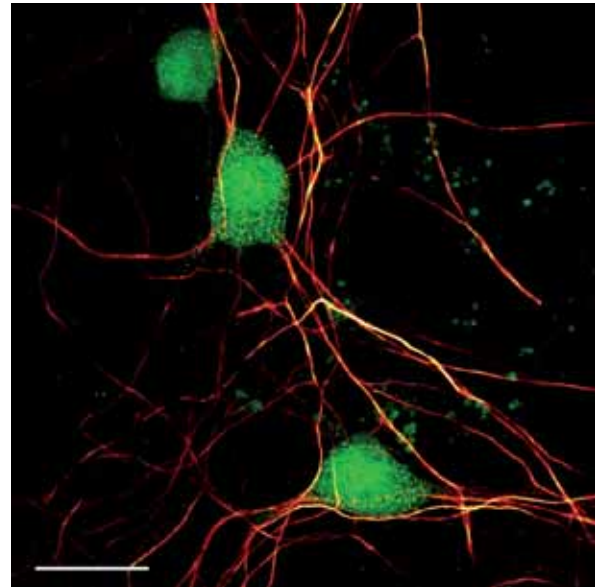


**Fig. 2.** Parvalbumin expressing neurons. Top: parvalbumin expressing neurons in cortical neuronal culture (28 DIV), green: Parvalbumin, red: NF 200, bar: 20  $\mu\text{m}$ . Bottom: axonal ramifications (arrows) of a parvalbumin expressing neuron, bar: 15  $\mu\text{m}$ .

**Acknowledgement**

This work was supported by the DFG-research training group *welisa* 1505/1 and grants of Mecklenburg-Western Pomerania (UR09045 of the Ministry of Education, Science and Culture, and V220-630-08-TFMV-F-011 (project part FLUXELL) of the Ministry for Economics, Work and Tourism).

**References**

[1] Marom S., Shahaf G. “ Development, learning and memory in large random networks of cortical neurons: lessons beyond anatomy” *Quarterly Reviews of Biophysics* 35 pp. 63 - 87, 2002

[2] Koester P. J., Buehler S. M., Stubbe M., Tautorat C., Niendorf M., Baumann W., and Gimsa J. (2010). Modular glass chip system measuring the electric activity and adhesion of neuronal cells – application and drug testing with sodium valproic acid. *Lab-chip*, DOI: 10.1039/b923687b.

# Long-term recordings from organotypic co-cultures of VTA-SN/PFC

Elena Dossi<sup>1\*</sup>, Francesca Gullo<sup>1</sup>, Claudia Heine<sup>2</sup>, Heike Franke<sup>2</sup>, Mariapia Abbracchio<sup>3</sup>, Peter Illes<sup>2</sup>, Enzo Wanke<sup>1</sup>

<sup>1</sup> Department of Biotechnology and Biosciences, University of Milan-Bicocca, Milan, Italy

<sup>2</sup> Rudolf-Boehm-Institute of Pharmacology and Toxicology, University of Leipzig, Leipzig, Germany

<sup>3</sup> Department of Pharmacological Sciences, Laboratory of Molecular and Cellular Pharmacology of Purinergic Transmission, University of Milan, Milan, Italy

\* Corresponding author. E-mail address: e.dossi@campus.unimib.it

We characterized the developmental and regeneration features of a brain circuitry involved in working memory (the ventral tegmental area-substantia nigra [VTA-SN] fibers projecting to the prefrontal cortex [PFC] and the complementary glutamatergic pathways). By utilizing a co-culture system adapted to multi electrode platforms (MEAs), we simultaneously recorded (and analyzed) both spikes and local field potential activity. After few days *in-vitro* (div) the co-cultures showed a spontaneous activity in the form of bursts, trains of action potentials, and LFPs, lasting ~0.3 and 1.5 s, respectively. At 6-7 div we observed that the activity increased in parallel with the growth of new projections from one slice to the other. We typically observed three types of activities organized as follows: 1) bursts only in VTA-SN, while PFC was silent, 2) bursts originating in VTA and rapidly reaching PFC, that is cross-correlated activity, and 3) bursts with synchronous activity in both regions. This correlated activity was completely abolished if new-born projections between the two areas were cut. Preliminary data suggest that the activity of the co-cultures is modulated by dopaminergic and GABAergic systems. In conclusion, the co-cultures of VTA-SN/PFC on MEAs represent a good and useful model to study the regenerative processes of neurons over time.

## 1 Introduction

The mesocorticolimbic system originates from the dopaminergic cell bodies of the mesencephalic ventral tegmental area/substantia nigra (VTA-SN) complex and projects to the prefrontal cortex (PFC), implicated in working memory, both in primates and in rodents. A feature common to many neurodegenerative diseases is the injury of the dopaminergic VTA-SN neurons with the consequence of affecting the activity of PFC neurons in different ways [1-3]. It has been demonstrated that organotypic slice cultures from VTA-SN and PFC can be used as an appropriate model to study the establishment and post-injury regeneration of dopaminergic fibers in this circuit [4,5].

## 2 Methods

Neonatal P1-2 mice pups have been used to prepare organotypic co-cultures as described [4,5]. Briefly, 200  $\mu$ m thick slices were placed side-by-side in sterile MEA petri dishes, previously coated with collagen (3,5 mg/mL, Millipore), and covered with gas permeable covers (MEA-MEM, Ala Scientific Instruments, Inc., USA). The culture medium was added to the slices up to an interface level [6,7] and changed daily. After 2-3 days *in vitro* (div), both local

field potentials (LFP) and spikes were acquired at 37°C in CO<sub>2</sub>-controlled incubators from MEA-1060BC preamplifiers (bandwidth 0,1-8 KHz, Multi Channel Systems, Germany) at 32 KHz and analyzed by using appropriate filters (LFP [0,1-200 Hz], spikes [0.25-5 KHz]) through MC\_Rack software (MEA64).

## 3 Results

After few days the co-cultures showed a spontaneous activity, characterized by bursts, trains of action potentials, and LFPs, lasting ~0.3 and 1.5 s, respectively. At 5-6 div (days *in vitro*) we observed that the activity of the co-cultures increased in parallel with the growth of new projections from one slice to the other: the bursting activity enhanced and, as it is possible to observe in Fig.1, the amplitude of LFPs increased during time both in VTA and PFC.

In each MEA it was possible to study a rich repertoire of activity, which consisted of bursts only in VTA, bursts originating in VTA *and* rapidly reaching PFC (with a delay of ~100-150 ms, depending on the time of culture, Fig.2), and bursts with synchronous activity in both regions. With the advancing of time in culture, there was also the appearance of bursts which started from the PFC and back-propagated to the VTA (Fig.2), in agreement

with the fact that almost all areas of the brain receiving projections from the VTA project back to it.

This correlated activity was completely abolished if the new-born projections between the two areas were cut.

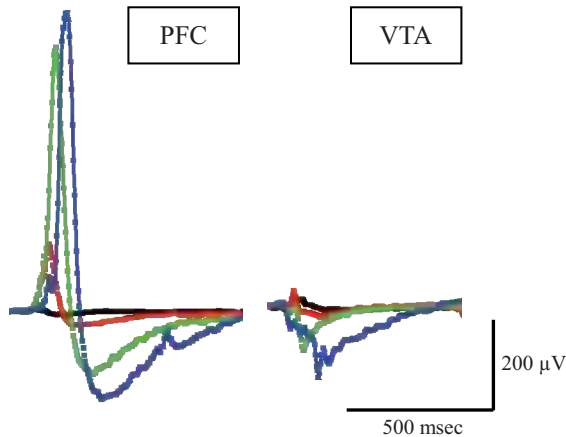


**Fig. 1.** Development of local field potentials in a VTA-SN/PFC co-culture. The traces are recorded at: 5 (black line), 10 (red line), 12 (green line) and 14 div (blue line) from two electrodes in PFC (left) and VTA (right).

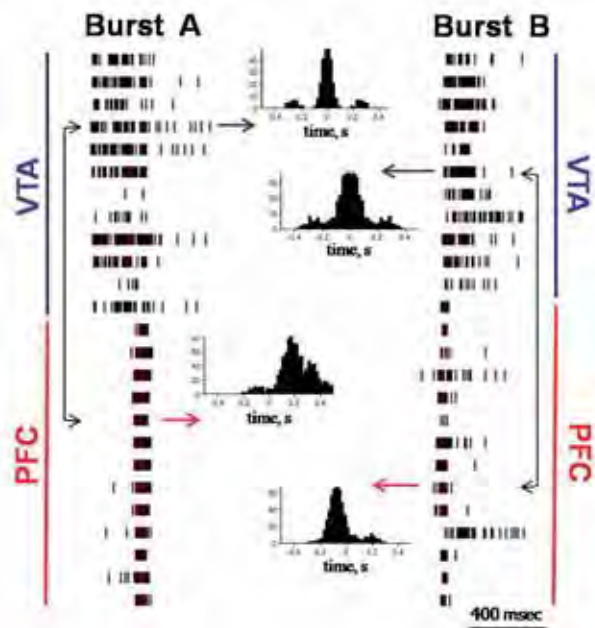


**Fig. 2.** Bursting activity of the VTA-SN/PFC co-cultures. On the left, example of a burst (burst A) originating from the VTA (blue) and propagating to the PFC (red); on the right, example of a burst (burst B) starting from the PFC (red) and back-propagating to the VTA (blue). In the middle, auto- (upper graphs) and cross- (lower graphs) correlograms of the activity from two electrodes in VTA (one from burst A and one from burst B), taken as references, and from two electrodes in PFC, during the two previously described bursts, respectively. From the first cross-correlogram, it is possible to appreciate the delay of the activity in PFC during the burst originating from the VTA, while the lower one shows that activity in the PFC can anticipate the activation of the VTA.

Preliminary pharmacological assays suggest a dopamine receptor dependence and a modulation mediated by the GABAergic system (Fig.3): the

treatment with specific agonists/antagonists of dopamine and GABA receptors modified the temporal patterns of the activity.

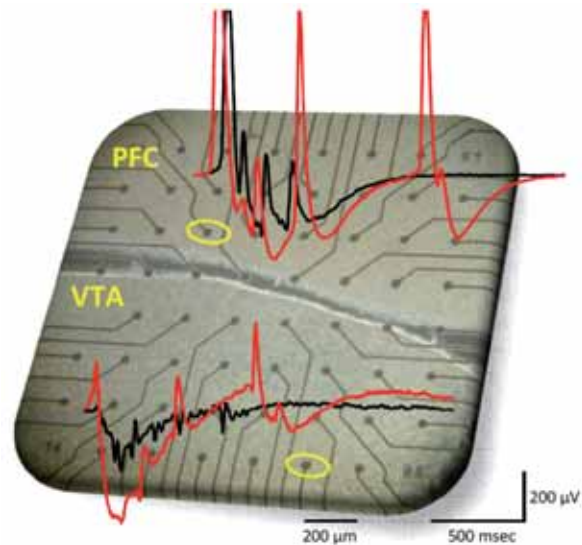


**Fig. 3.** Representative co-culture of VTA-SN/PFC on Multielectrode Arrays. Examples of LFPs recorded in control (black traces) and in presence of 3µM gabazine (red traces) from two electrodes (yellow circles) in PFC and VTA.

## 4 Conclusions

In conclusion the co-cultures of VTA-SN/PFC on MEAs represent a good model and an useful and powerful tool to study the neuronal regenerative processes and their functionality over time; moreover, it enables us to analyse how these processes are influenced by the application of detrimental (toxic/hypoxic) stimuli or implemented by potentially interesting “trophic” and novel neuro-reparative substances.

We will also exploit the ability of endogenous stem/precursor cells of brain parenchyma to sustain the regeneration-remodeling of damaged circuitries and to possibly differentiate to new-born neurons and glia able to replace irreversibly damaged cells.

## Acknowledgement

This study was supported by a grant from *Cariplo Foundation* to EW, MA and PI.

## References

- [1] Gullledge and Jaffe, (2001), *J. Neurophysiol.*, 86:586-595.
- [2] Seamans et al., (2001), *J. Neurosci.*, 21(10):3628-3638;
- [3] Cepeda et al., (1992), *Synapse*, 11:330-341.
- [4] Heine et al., (2007), *Neurosci.*, 149:165-181.
- [5] Franke et al., (2003), *Neurochem. Int.*, 42:431-439.
- [6] Maeda T. et al., (2004), *Brain Res.*, 1015:34-40.
- [7] Shimono K. et al., (2002), *J. Neurosci. Meth.*, 120:193-202.

# Identification of Local Field Potentials and Spikes on MEA256 Platforms

Gullo Francesca, Maffezzoli Andrea, Dossi Elena, Wanke Enzo\*

Department of Biotechnologies and Biosciences, University of Milano-Bicocca, Milan, Italy

\* Corresponding author. E-mail address: enzo.wanke@unimib.it

The neural signals recorded extracellularly consist of fast time-varying action potentials (“spikes”) superimposed on relatively slow and field potentials (LFP). Usually, the former type of activity, known as multiple-unit activity (MUA), can be waveform-sorted if the recording electrodes are sufficiently small and estimated in the high-frequency range (typically 200–5000 Hz), whereas the LFPs are assessed in the low-frequency range (e.g., 1–150 Hz) (Menendez de la Prida L et al., *Neuron* 2006; 49:131-142.). Here we suggest that a very low frequency component of the recorded LFPs originates from diffusion potentials and is not produced by synaptic or voltage-gated ion channels currents.

## 1 Background

A large number of experiments have suggested that single-unit spikes are primarily attributable to spiking activity of pyramidal or inhibitory neurons, and thus measure the cortical output (Barthò et al., *J. Neurophysiol.* 2004; 92:600-608.). On the other hand, LFPs probably reflect synaptic currents (Belitski et al., *J. Neurosci.* 2008;28:5696-5709.), including voltage-dependent membrane oscillations and slow ion diffusion potentials caused by momentary changes of extracellular concentrations around cells (Bedard et al., *Biophys. J.* 96:2589-2603, 2009; Pettersen et al., *J. Comput. Neurosci.* 24:291-313, 2008). The ion diffusion had been studied in detail in cerebellar tissue and it was found that it can be characterized by the volume fraction ( $\alpha$ ) and tortuosity ( $\lambda$ ) that represent the fraction of extracellular volume relative to that of the whole tissue and the complexity of all the cells that impede diffusion, respectively. It resulted that with respect to simple physiological solution, the extracellular space occupies about 20 % of the cerebellum and that the diffusion coefficient for small monovalent extracellular ions is reduced by a factor of 2.4, the time course of diffusion changes and the overall effect is to increase the apparent strength of any ionic source 12-fold (Nicholson and Phillips, *J. Physiol.* 321:225-257, 1981).

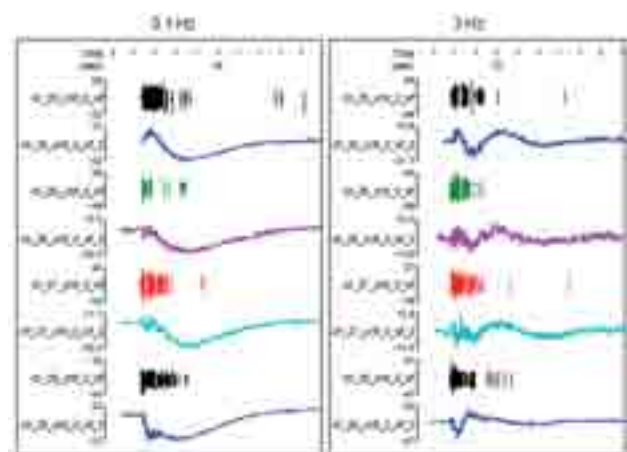
## 2 Methods

Here we report results obtained by using the multi-electrode array (MEA, 250 electrodes, MCS, Reutlingen, Germany) simultaneous recordings from reverberating postnatal neocortical long-term cultured networks with excitatory/inhibitory ratios typical of intact tissue. After separating spikes from LFPs by appropriate filters we adopted classical spike sorting techniques for identifying clusters of excitatory and

inhibitory cells (Gullo et al., 2009; *J Neurosci Methods* 181:186-198; *Frontiers Neural Circuits*, April, 2010). In brief we used the autocorrelation function (AC) and other statistical features (ISI, Fano factor, etc) of each waveform-identified neuron to find appropriate clusters of cells characterized by similar activity. Recordings of LFPs from MEA256 amplifiers results in waveforms that have a low frequency of 1 Hz (3 RC, 1 pole filter). But we evaluated also data recorded with a MEA64 system from a 0.1 RC-1 pole and 3 Hz Bessel-4 pole low cut.

## 3 Results

We compared LFP data and spikes firing for each identified neuron during each burst from each electrode. To evaluate the relevance of the synaptic

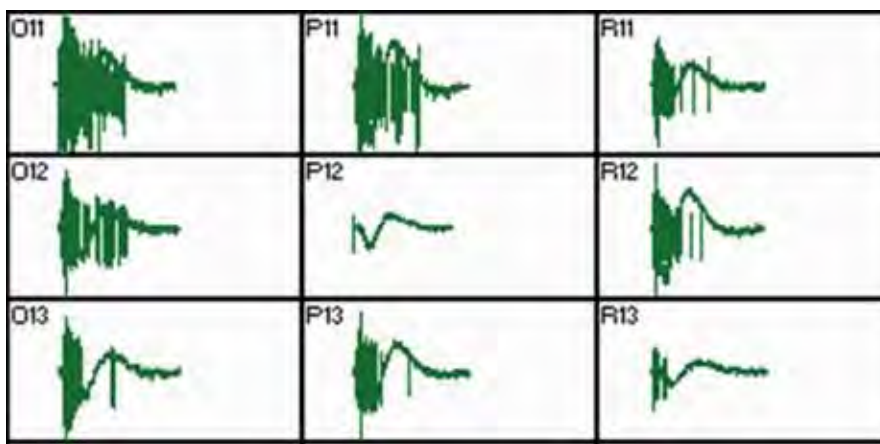


current and ion diffusion in LFP data, we compared recordings, obtained either with a low cut-off at 0.1 or 3 Hz. As shown in the upper figure (time scale 1 s, y-scale,  $\mu\text{V}$ ), the LFPs recorded with the 0.1 Hz filter are mainly negative-going with a 0.5 s duration, contrary to those recorded with the 3 Hz filter which show an oscillatory behaviour. Such a response is

indeed expected and is due to the 3 Hz filter properties. Furthermore, to clarify which is the origin of such low components we could find amongst 252 electrodes (MEA256, 1 Hz, 3 RC-1pole cut-off) some that were: 1) devoid of spikes but with LFPs and therefore in principle devoid also of synaptic currents, but 2) surrounded by electrodes with spikes and LFPs. In the figure shown below (time scale 5 s,  $\pm 100 \mu\text{V}$ ), P12 is such an electrode and all the others have LFPs and spikes (here superimposed). It can be seen that the LFP present in P12 is a delayed and small combination of those present in the neighbouring electrodes, thus suggesting that these low frequency components simply derive by the surrounding diffusion-induced

## 4 Conclusions

These results together with preliminary observations of bursts spread at a speed of  $\sim 10 \text{ mm/s}$  in the large culture area ( $9 \text{ mm}^2$ ) should also help new studies on the origin of cortical spreading depression which has been observed in during aura in familial hemiplegic migraine patients (Tottene et al., *Neuron* 61:762-773, 2009). The application of these results on cultured networks from knock-in human-mutations engineered mice and related pharmacological manipulation should advance the evaluation of therapeutic drugs.



current and diffusion are present. Furthermore, to cancel these unwanted components (without touching the fast synaptic components related directly to firing) we searched the lowest frequency at which a high-pass

Bessel filter (8 poles) produces an almost complete cancellation and it resulted that this frequency is around  $3/4 \text{ Hz}$ . This value agrees with the simplest application of the Fick 2nd law of diffusion ( $\langle x^2 \rangle = D \cdot t$ ) that tells us that the average duration of a concentration change in a  $100 \mu\text{m}$  distance is about  $1.6 \text{ s}$  ( $D = 10^{-5} \text{ cm}^2 \cdot \text{sec}^{-1}$ ).



# Up/down States Synchrony Studied in Cortical Networks: Roles of Ion Channels, Neurotransmitter Transporters and GABA Receptors

Gullo Francesca, Maffezzoli Andrea, Dossi Elena, Wanke Enzo\*

Department of Biotechnologies and Biosciences, University of Milano-Bicocca, Milan, Italy

\* Corresponding author. E-mail address: enzo.wanke@unimib.it

It has been shown by single-cell and multiunit electrophysiology in layer III entorhinal cortex and disinhibited hippocampal CA3 slices that the balancing of the up-down activity is characterized by both GABA<sub>A</sub> and GABA<sub>B</sub> mechanisms. Here we report novel results obtained using multi-electrode array (MEA, 60 electrodes) simultaneous recordings from reverberating postnatal neocortical networks. Concentration-response pharmacology of up- and down-state lifetimes in clusters of excitatory (n=1067) and inhibitory (n=305) cells suggests that, besides the GABA<sub>A</sub> and GABA<sub>B</sub> mechanisms, others such as GAT-1-mediated uptake, I<sub>h</sub>, I<sub>NaP</sub> and I<sub>M</sub> ion channel activity, robustly govern both up- and down-activity. These results should reinforce not only the role of synchrony in CNS networks, but also the recognized analogies between the Hodgkin-Huxley action potential and the population bursts as basic mechanisms for originating membrane excitability and CNS network synchronization, respectively.

## 1 Background/Aims

Action potential propagation and synaptic transmission are shared by both peripheral and central nervous systems to sustain fast responding excitability. Nevertheless, both systems are constitutively acted upon by several fundamental but conflicting properties such as serial or parallel activity, rate or temporal spike coding, independent or synchronous operation, reliable or unreliable synaptic transmission, respectively (1). It has been shown by single-cell and multiunit electrophysiology in layer III entorhinal cortex and disinhibited hippocampal CA3 slices that the balancing of the up-down activity is characterized by both GABA<sub>A</sub> and GABA<sub>B</sub> mechanisms (2, 3). [1].

## 2 Methods

Here we report novel results obtained using multi-electrode array (MEA, 60 electrodes) simultaneous recordings from reverberating postnatal neocortical networks containing 19.2±1.4% GABAergic neurons, typical of intact tissue. We provided evidence (4) that the autocorrelation function (AC) (and other statistical features) of each identified neuron represents a very good model to find appropriate clusters of cells characterized by similar activity. For each cluster, identified by standard K-means procedures using the Principal Component Analysis (PCA) of AC components, we computed physiological parameters such as burst duration (BD), number of spikes in each burst (SN), average interburst spike rate (IBSR), inter burst intervals (IBI)

which, indeed, resulted to be very different in each cluster. On the whole, it resulted that the initial sorting into units unveiled intrinsic multiplicity of responses of assemblies of cells during pharmacological manipulations.

## 3 Results

We observed that in each spontaneous up-state (burst) the total number of spikes in identified clusters of excitatory and inhibitory neurons is almost equal, thus suggesting a balanced average activity. Interestingly, during the early up-state phase, firing rate is sustained by only 10 % of the total spikes but grows in a regenerative mode reaching a peak at 35 ms with the number of excitatory spikes greater than inhibitory, therefore indicating an early unbalance. Concentration-response pharmacology of up- and down-state lifetimes in clusters of excitatory (n=891) and inhibitory (n=237) cells suggests that up- and down network states (here quantified by BD and IBI, respectively) not only depend on GABA<sub>A</sub> and GABA<sub>B</sub> receptors as already reported (2, 3), but also on pacing and spike frequency accommodation currents (i.e. I<sub>h</sub> and I<sub>M</sub>, respectively). To investigate the role of the pacemaker currents we used an I<sub>h</sub> blocker (ZD7288). To remove the steady-state inhibition, we first disinhibited the network with a maximal concentration of gabazine (10 μM) and then applied on top increasing ZD concentrations. Under these conditions we further clarified if the role of I<sub>h</sub> is different between inhibitory or excitatory neurons. As shown in the figure, increasing ZD concentrations produced a net BD decrease and IBI increase up to a total and

completely reversible block of activity, suggesting a crucial role for this current. Both the BD and IBI effects seem to operate approximately at the same ZD concentration of about 30  $\mu\text{M}$ . With the aim of clarifying the mechanism of the BD decrease in one (out of 3) experiments, we show in C the cumulative histograms of BD under control (thin line), in 10  $\mu\text{M}$  GBZ (medium line) and 10  $\mu\text{M}$  GBZ in the presence of 10  $\mu\text{M}$  ZD (thick line). These data (follow the arrows) show the effect of disinhibition and blockade of  $I_h$  which produced a large increase and a strong shortening in the burst duration, respectively ( $p < 0.02$  for all of the 15 pairs, excitatory/inhibitory, control/GBZ/GBZ+ZD). The burst structure analysis was performed in the same three conditions and is shown in D in the form of neuron-SR (spike rate), because the cluster data were divided by the number of cells and error bars have been added to illustrate the error arising at level of single cells data. It illustrates not only the typical effect of disinhibition, but also how ZD is able to remove it completely. In the inset, the difference of the cluster-SRs clearly illustrates that under the three different conditions the activity of the up-states can be completely altered by pharmacological manipulations.

## 4 Conclusions

These results should reinforce not only the role of synchrony in CNS networks, but also the recognized analogies between the Hodgkin-Huxley action potential and the population bursts as basic mechanisms for originating membrane excitability and CNS network synchronization, respectively (2).

## References

- [1] Lisman JE Trends Neurosci 1997;20:38-43.
- [2] Menendez de la Prida et al., Neuron 2006; 49:131-142.
- [3] Mann et al., J. Neurosci. 2009;29:7513-7518.
- [4] Gullo et al., 2009; J Neurosci Meth 181:186-198; Gullo et al., Front. Neural Circuits 2010/04

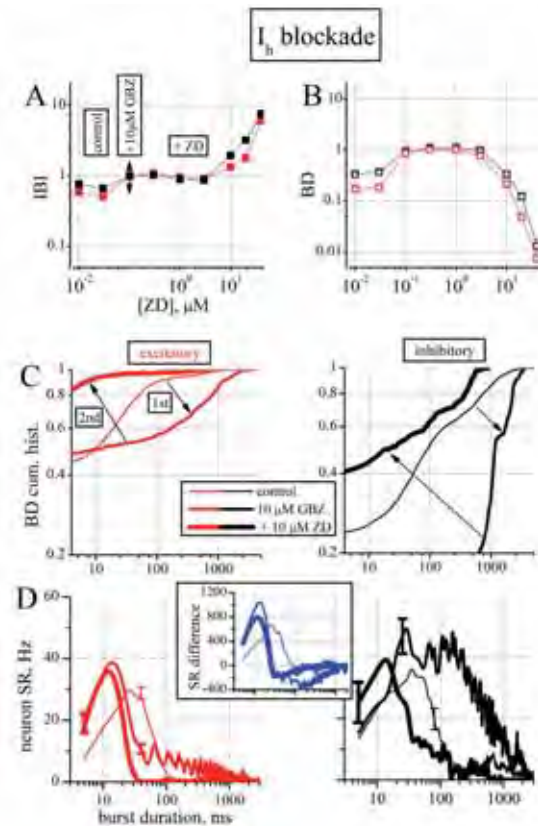


**Fig. 1. The effects of blocking  $I_h$  (with ZD7288)** A-D) Effects of ZD. A, B) Dose-response curves for IBI and BD evaluated for the excitatory (red symbols) and inhibitory (black symbols) cluster of neurons (total number of cells: 192, 45, respectively). C) BD cumulative histogram data from one of the 3 experiments with 36 excitatory (left) and 13 inhibitory (right) cells. Arrows indicate the temporal sequence during the experiment. For the single experiment shown, mean values of IBI and BD (in parenthesis the inhibitory cells) in control were, respectively:  $8.3 \pm 0.3$  s, ( $7.4 \pm 0.3$ );  $61 \pm 7$  ms ( $405 \pm 68$ ),  $n=36$  ( $n=13$ ). The values in 10  $\mu\text{M}$  GBZ were:  $10.2 \pm 0.4$  s, ( $15.5 \pm 0.6$ );  $374 \pm 60$  ms ( $1430 \pm 0.8$ ) and in 10  $\mu\text{M}$  ZD were:  $22.2 \pm 1.3$  s, ( $19.2 \pm 0.75$ );  $70 \pm 17$  ms ( $450 \pm 61$ ). D) nSR (neuron-normalized cSR in each cluster) is plotted vs. burst duration, for excitatory (left) and inhibitory (right) typical cells. Thin, medium and thick lines are used to distinguish control, 10  $\mu\text{M}$  GBZ and 10  $\mu\text{M}$  ZD on top, respectively. Inset illustrates the cSR difference between excitatory and inhibitory clusters.

# From Neuron to Network: The Roles of Synaptic Proteins in Neuronal Network Activity

Lavi Ayal<sup>1</sup>, Sheinin Anton<sup>1</sup>, Ashery Uri<sup>1\*</sup>

<sup>1</sup> Department of Neurobiology, Life Sciences Faculty, Tel Aviv University, Israel

\* Corresponding author E-mail address: uriashery@gmail.com

We have developed a novel platform to study the effects of genetic manipulations, such as overexpression or knock-down, on the spontaneous activity of neuronal networks. A combination of viral infection and fluorescent time-lapse imaging is employed to study the kinetics of the overexpression and the effects are measured using MicroElectrode Array (MEA) recordings. Our preliminary results show that manipulations of specific synaptic proteins alter the spike bursting activity of dissociated cortical neuronal networks.

## 1 Introduction

The plasticity of the brain plays a key role in shaping our behavior, learning and memory. It is well known that plasticity is associated with alteration in synaptic strength and efficacy. Some of these effects correlate with changes in the levels of synaptic proteins [1]. However, the implications of genetic alteration in synaptic proteins on the network activity of neurons are not known. We examine the effects of DOC2B, a synaptic neuronal  $Ca^{2+}$  sensor that enhances exocytosis and vesicle refilling, on spontaneous network activity expecting to detect a role in neurons during high frequency stimulation periods [2].

## 2 Methods

We use MicroElectrode Array (MEA) technology to simultaneously record action potentials from multiple neurons in *ex vivo* neuronal network. Cortical murine neurons are extracted from postnatal mice and plated at a density of  $\sim 3000$  cell/mm<sup>2</sup>. Experiments are performed 12-14 days after dissection. Proteins overexpression is achieved by viral infection and fluorescent-microscopy combined with long-term time-lapse imaging is employed to study the kinetics of the overexpression (Fig. 1).

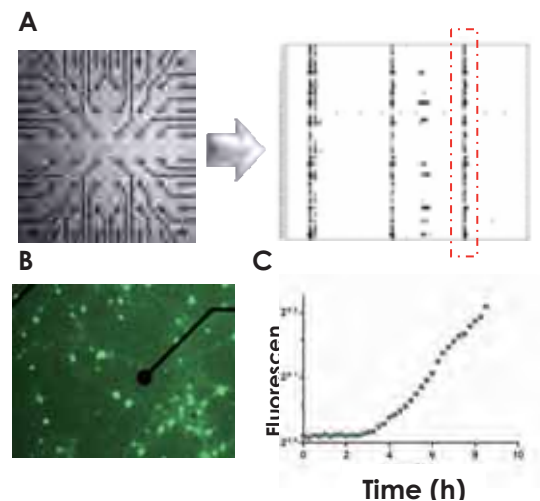


**Fig. 1.** Recording from a neuronal network on a Micro-Electrode Array (MEA) overexpressing DOC2B. We established the MEA recording system (A, left) and successfully recorded different patterns of spontaneous burst activity (A, right). Each bar corresponds to a spike in a single neuron. One of the bursts is boxed in red. (B) Neurons expressing DOC2B-IRES-EGFP. In addition, the expression efficiency of DOC2B was found to be very high, starting as early as 3-5 h after infection (C).

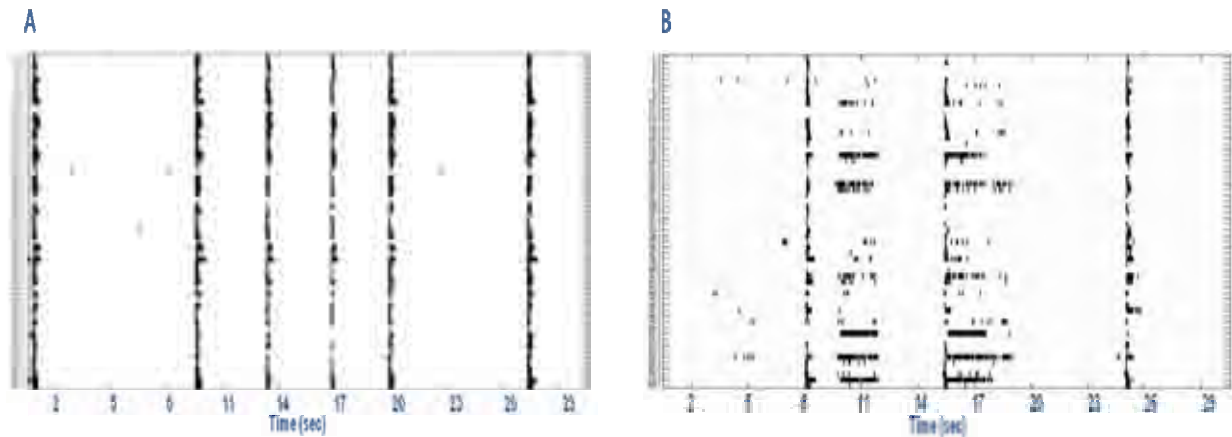


**Fig. 2.** DOC2B overexpression induces an increase in burst duration. Burst duration begins to significantly increase ~5 h after DOC2B introduction. GFP-overexpressing networks showed no change in these parameters (not shown). Raster plots of spontaneous activity before (A) and after (B) overexpression of DOC2B.

### 3 Results and Discussion

Overexpression of DOC2B leads to a distinctive increase in the durations of neuronal network spikes bursting activities (Fig. 2). This unique combination of genetic manipulation on the neuronal network level complements and extends our understandings of the role of DOC2B in synaptic transmission. It has been previously suggested that synchronized bursting activities may be templates for modifications of network-wide neuronal plasticity. Together, we suggest a novel role for DOC2B – tuning of synaptic plasticity to allow imprint of activity patterns.

#### Acknowledgements

We thank The Joan and Jaime Constantiner Institute for Molecular Genetics, The Rabin Institute for Neurobiology and the Adams Super Center for Brain Studies for participating in financial support.

#### References

- [1] Littleton, J.T., Bai, J., Vyas, B., Desai, R., Baltus, A.E., Garment, M.B., Carlson, S.D., Ganetzky, B., and Chapman, E.R. (2001). synaptotagmin mutants reveal essential functions for the C2B domain in Ca<sup>2+</sup>-triggered fusion and recycling of synaptic vesicles in vivo. *J Neurosci* 21, 1421-1433.
- [2] Friedrich, R., Groffen, A.J., Connell, E., van Weering, J.R., Gutman, O., Henis, Y.I., Davletov, B., and Ashery, U. (2008). DOC2B acts as a calcium switch and enhances vesicle fusion. *J Neurosci* 28, 6794-6806.

# Chronic network stimulation enhances spontaneous spike rates

Gregory J. Brewer<sup>1</sup>, Michael D. Boehler<sup>1</sup>, R A Pearson<sup>1</sup>, A A DeMaris<sup>1</sup>, A N Ide<sup>1</sup>, Bruce C. Wheeler<sup>2</sup>

<sup>1</sup> Southern Illinois University School of Medicine, Springfield, IL USA

<sup>2</sup> University of Florida, Gainesville, FL USA

Neurons cultured on multielectrode arrays almost always lack external stimulation except during the acute experimental phase. We have investigated the effects of chronic stimulation during the course of development in cultured hippocampal neural networks by applying paired pulses at half of the electrodes for 0, 1 or 3 hr/day for 8 days. Spike latencies increased from 4 to 16 ms as the distance from the stimulus increased from 200 to 1700  $\mu\text{m}$ , suggesting an average of four synapses over this distance. Compared to no chronic stimulation, our results indicate that chronic stimulation increased evoked spike counts per stimulus by 50% at recording sites near the stimulating electrode and increased the instantaneous firing rate. On trials where both pulses elicited responses, spike count was 40-80% higher than when only one of the pulses elicited a response. In attempts to identify spike amplitude plasticity, we found mainly amplitude variation with different latencies suggesting recordings from neurons with different identities. These data suggest plastic network changes induced by chronic stimulation that enhance the reliability of information transmission and the efficiency of multisynaptic network communication.

## 1 Background/Aims

A key reason for low spontaneous spike rates of neuronal cultures may be caused by a sleeping or catatonic network which receives no external stimulation. Our work was motivated by the network studies of Potter (Wagenaar et al., 2005) who showed that burst dynamics can be greatly modulated by repeated high frequency stimulation, but chronic stimulation over many days was not investigated. We pose two alternative hypotheses applied to cultured networks. 1) Paired-pulse stimulation over long periods (chronic stimulation), will reduce spontaneous bursting, but increase overall spike rates similar to acute high frequency stimulation. Or, 2) Chronic paired-pulse stimulation will increase spontaneous spike rates possibly within a burst. Here we report a major effect of chronic stimulation on spontaneous spike rates and burst dynamics during two-weeks of network development in vitro.

## 2 Methods

E18 rat hippocampal cells were plated at 500 cells/mm<sup>2</sup> on poly-D-lysine coated MEAs in NbActiv4<sup>®</sup> medium (Brewer et al., 2008; Brewer et al., 2009) (BrainBits, Springfield, IL) Spikes were analyzed within a 2 ms search window for their peak-to-peak amplitudes and detections were noted whenever the peak-to-peak amplitude exceeded 11 times the noise standard deviation. Stimulation trains for chronic stimulation included groups of 30  $\mu\text{A}$  paired pulses (50 ms ISI; biphasic, 100  $\mu\text{s}$ /phase duration, positive first) with a wait of 5 seconds

between pairs. Arrays were chronically stimulated for either 0, 1 or 3 hour(s)/day at 7, 11, 12, 14, 18, 19, and 21 days in vitro. An automatic stimulation program stimulated the entire top half of the MEA (30 electrodes) in a pseudorandom sequence. The bottom half of the array never received direct stimulation from an adjacent electrode. A burst was defined as a sequence of at least 5 spikes with interspike interval less than 100 ms. Burst analyses were conducted with MatLab software with a burst criterion of  $> 0.4$  bursts/min.

## 3 Results

### 3.1 Effect of chronic stimulation on spontaneous activity

Compared to the customary procedure with no chronic stimulation during culture, chronic stimulation for 1 hr/day x 8 days resulted in higher overall spike rates and more active electrodes, mostly in barrages of activity called bursts.

### 3.2 Burst analysis

The frequency of spontaneous spikes occurring within a burst was seen to increase with duration of chronic stimulation (Fig. 1). The intra-burst spiking frequency of 93 Hz in networks stimulated for 3 hr/day during culture development was 2-fold higher than networks without chronic stimulation at 45 Hz and 1.4-fold higher than cultures chronically stimulated for 1 hr, 64 Hz. This was accompanied by an increase in spikes per burst for 1 hr/day chronic

stimulation/day but a reduction for 3 hr/day stimulation. While the frequency of spikes within a burst was highest in cultures chronically stimulated for 3 hr, these networks had the lowest burst duration, about 100 ms less than cultures stimulated for 0 or 1 hr/day. Cultures chronically stimulated for 1h had the longest burst duration of 400 ms which was 50 ms longer than the unstimulated condition. The percentage of electrodes with bursting activity nearly doubled in arrays chronically stimulated for 1 hr/day compared to the unstimulated condition. The majority of spikes occurred within bursts; electrodes with non-bursting spikes accounted for less than ten percent of the total active electrodes for all conditions. Total spike rates, burst spike rates and non-burst spike rates were nearly 2-fold higher for 1hr/day compared to the unstimulated condition and cultures stimulated 3 hr/day. Non-burst spike rates were consistently about 10% of the burst spike rates, consistent with the percent non bursting electrodes.

### 3.3 Overall spike rates and active electrodes

The overall spike rate of bursts and single spikes for cultures chronically stimulated for 1 hr/day was 2-fold higher than unstimulated cultures, but also higher than cultures stimulated for 3hr. Cultures chronically stimulated for 1 or 3 hr/day also have 30-50% more active electrodes than the unstimulated condition.

### 3.4 Impact of nearest neighbors

There is no simple, consistent relationship between spike rate and either stimulation proximity or duration of chronic stimulation. For 1 hour stimulation, activity decreased with the number of adjacent stimulation electrodes, consistent with the second hypothesis above. But with 3 hour stimulation, activity increased, albeit modestly, consistent with the first hypothesis.

## 4 Conclusions/Summary

Chronic stimulation of planar hippocampal networks on MEAs during the course of culture results in more spontaneous activity than unstimulated cultures, with higher spike rates within bursts. Thus, chronic stimulation changes the dynamics of the network so that proximity to stimulus is no longer the most important determinant of spike rate.

### Acknowledgements

This work was supported in part by NIH NS052233 from the National Institute of Neurological Sciences. We thank Professor Martinoia's lab for providing the spike/burst detection algorithm.

### Published reference

Brewer GJ, Boehler MD, Ide AN and Wheeler BC. Chronic electrical stimulation of cultured hippocampal networks increases spontaneous spike rates. *J Neurosci Meth* 2009; 184: 104-109.

Conflict of interest: Brewer receives royalties from invention of Neurobasal, B27 (trademarks of Invitrogen) and NbActiv4®. He also owns BrainBits LLC, the manufacturer and supplier of NbActiv4.

### References

- [1] Brewer, M. D. Boehler, T. T. Jones, and B. C. Wheeler. NbActiv4 medium improvement to Neurobasal/B27 increases neuron synapse densities and network spike rates on multielectrode arrays. *J Neurosci. Methods* 170:181-187, 2008.
- [2] Brewer, M. D. Boehler, R. A. Pearson, A. A. Demaris, A. N. Ide, and B. C. Wheeler. Neuron network activity scales exponentially with synapse density. *J Neural Eng* 6:14001, 2009.
- [3] Wagenaar, R. Madhavan, J. Pine, and S. M. Potter. Controlling bursting in cortical cultures with closed-loop multi-electrode stimulation. *J Neurosci* 25:680-688, 2005.

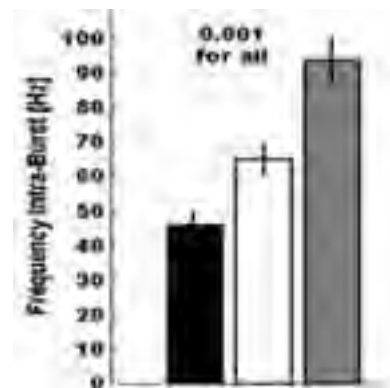


Fig. 1: Spike rate within bursts for 5 electrode arrays stimulated for 0 (black), 1 (white) or 3 hr./day (gray).

# Toward panneuronal recording of multisensory information processing in the medicinal leech

Daniel A. Wagenaar<sup>1\*</sup>, John Nagarah<sup>1</sup>, Pieter Laurens Baljon<sup>1,2</sup>, and Cynthia Harley<sup>1</sup>

<sup>1</sup> California Institute of Technology, Broad Fellows Program and Division of Biology, Pasadena CA, USA

<sup>2</sup> Vrije Universiteit, Amsterdam, The Netherlands

\* Corresponding author. E-mail address: daw@caltech.edu

Medicinal leeches use both visual and mechanosensory information to guide them toward their prey. We are interested in how they integrate these two streams of information in their nervous system. We approach this question both using behavioural experiments and using recordings from the segmental nervous system. In particular, we are developing a unique combination of custom multielectrode arrays and voltage-sensitive dyes to record in parallel from very many (ultimately perhaps even all) cells in a segmental ganglion. This poster will present an overview of the work in the lab; more technical details will be presented on separate posters by Pieter Laurens Baljon [1] and John Nagarah [2].

## 1 Background/Aims

What if you could record action potentials simultaneously from every single neuron in a brain area? This dream could soon be a reality for the segmental ganglia of the medicinal leech (Fig. 1). Our lab studies how information from visual and mechanosensory sensilla are combined in the leech's CNS to allow the animal to form a coherent percept of prey location. Whereas higher animals (mammals, birds) have evolved complex circuitry involving multiple large brain areas to perform this

“multisensory integration”, the leech has only 400 neurons in its segmental ganglia, and only some of those are likely to be involved in prey localization. Behavioural studies have demonstrated that leeches do indeed use both sensory modalities to guide their actions, making these animals—with their exceptionally accessible nervous systems—ideal models to study the fundamentals of multisensory integration.

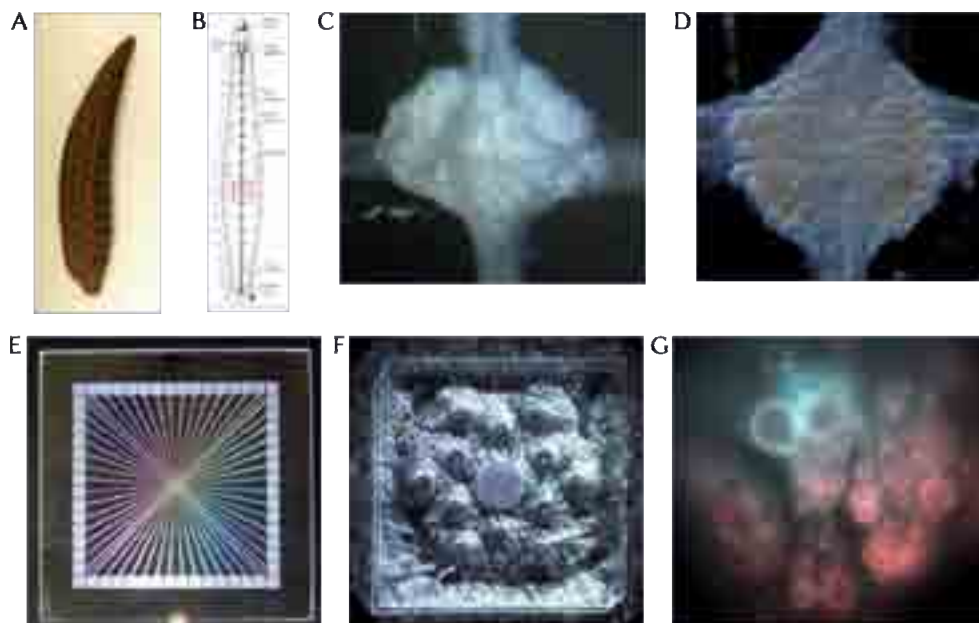
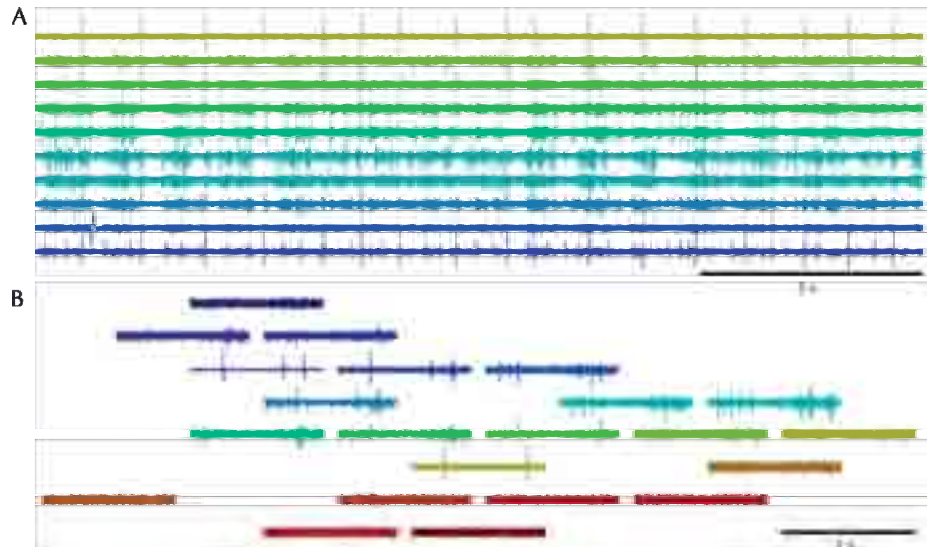


**Fig. 1.** A A medicinal leech. (Length: 10 cm) B Schematic of its nervous system. One ganglion is indicated. C Ventral aspect of a ganglion. (Diameter: 0.6 mm) D Dorsal aspect. E Prototype of MEA with ITO electrode leads, optimized for recording from leech. (Fits in MCS pre-amplifier) F Prototype of suction device. G Ventral aspect of ganglion visualized with voltage sensitive dyes (overlay of FRET donor in cyan and acceptor in red).

**Fig. 2.** Extracellular recording from one segmental ganglion within a nearly-whole leech nerve cord using a prototype custom MEA.

A A 20-second segment of a recording, showing periodic multielectrode bursting. B A shorter segment of the recording, with traces laid out according to electrode geometry.



## 2 Methods/Statistics

To make it possible to record action potentials from every single cell in the ganglion, we combine two powerful techniques: The first, voltage sensitive dye (VSD) imaging allows measurement of intracellular voltage changes in any number of neurons simultaneously, but with limited temporal resolution. The second, multielectrode array (MEA) recording, offers excellent temporal resolution, but does not ordinarily allow identification of individual cells in the recorded spike trains. We have built a dual-headed microscope that allows VSD imaging from both sides of the ganglion simultaneously. We are developing a spike sorting algorithm that combines spatial information from the VSD images with temporal information from the MEA recording so that spikes can be assigned to specific neurons with confidence [1]. In addition, we are developing MEAs with ring-shaped electrodes around suction holes to achieve near one-to-one contact between electrodes and cells [2].

## 3 Results

Imaging leech ganglia with VSDs is now a well-established technique (e.g. [3], and [1]). We have recently obtained the first MEA recordings from this preparation, both with commercial MEAs [1], and with our new custom MEAs [2]. Spontaneous activity in the leech nervous system (Fig. 2A) bears a striking resemblance to the well-known bursting pattern of dissociated cortical cultures (e.g. [4]). Closer examination (Fig. 2B) reveals that electrodes register signals from multiple neurons that participate in the activity, and that many neurons produce signals on multiple electrodes, making such recordings fertile ground for testing advanced spike sorting algorithms.

## 4 Conclusion/Summary

We have demonstrated that our MEAs [2] can record spiking activity from multiple sources within the leech ganglion, and that this recording method can be combined with simultaneous VSD recording [1], thus laying the groundwork for network-level studies of information processing.

### Acknowledgements

This presentation is partly based on work by John Nagarah and Pieter Laurens Baljon. Please refer to their posters for more details. Funding was provided by the Broad Foundations. DAW is a recipient of a Career Award at the Scientific Interface from the Burroughs-Wellcome Fund.

### References

- [1] P. L. Baljon, J. Nagarah, and D. A. Wagenaar, 2010. Poster at this conference.
- [2] J. Nagarah, P.L. Baljon, and D. A. Wagenaar, 2010. Poster at this conference.
- [3] S. M. Baca, A. Marin-Burgin, D. A. Wagenaar, and W. B. Kristan, 2008. *Neuron* 57, 276–289.
- [4] D. A. Wagenaar, J. Pine, and S. M. Potter, 2006. *BMC Neurosci.* 7, art. no. 11.



# Calcium dynamics during bursting activity in neocortical cultures

Matthew Goddard<sup>1\*</sup>, Ulrich Egert<sup>1,2</sup>

<sup>1</sup> Bernstein Center Freiburg, Univ. of Freiburg, Germany

<sup>2</sup> IMTEK - Department of Microsystems Engineering, Univ. of Freiburg, Germany

\* Corresponding author. E-mail address: matthew.goddard@bcf.uni-freiburg.de

Calcium influx during periods of bursting activity in primary dissociated cortical cultures was investigated. We used a marker for live cell calcium imaging combined with MEA recordings in 21-53 DIV cultures and found that multi-electrode site bursting, rather than single spikes, were associated with calcium transients during spontaneous network activity. Furthermore, spatio-temporal cell firing patterns tended to be conserved during bursts, despite subtle differences in burst propagation patterns.

## 1 Introduction

### 1.1 Calcium and signalling

Calcium ( $\text{Ca}^{2+}$ ) imaging of neural cells provides a useful measure of cell excitability, for example in the detection of action potentials [1, 2, 3], as well offering the capability for sampling at a high spatial resolution (e.g., up to  $610 \text{ mm}^2$  at 10x magnification, [4]). Recently it was shown that  $\text{Ca}^{2+}$  transients in cultured networks are reliably coupled to bursts, and that strength of this coupling is modified by the age of the culture [5]. However, it is also known that network firing activity and burst properties, such as burst duration and electrode participation, depend on a number of factors including seeding density [6]. In the present study one of the aims was to characterise in greater detail the relationship between peri-burst calcium transients in young (2-3 wks) and old (>7 wks) cultures with comparable seeding densities. We also sought to explore the dynamics of individual cell recruitment during bursts and how this may be modified by factors such as distance to burst onset, burst propagation, and electrode site recruitment (i.e., size of network burst). Glial cell calcium transients were of particular interest because of the capacity of glia to modulate neuronal activity [7]. Thus, as a final objective, we characterised peri-burst calcium transients in astrocytes as well as neurons [4, 8].

## 2 Methods

### 2.1 Cultures

Neocortical tissue was harvested from Wistar rat pups at PN0. Cortical cells were dissociated and cultured on  $6 \times 10$  (500/30) or  $8 \times 8$  (200/30) MEAs

at an initial density of approx. 6000 cells/ $\text{mm}^2$  for up to 53 days in vitro (DIV).

### 2.2 Calcium imaging

Cultures were bulk-loaded with  $9 \text{ }\mu\text{M}$  Fluo4AM (Molecular Probes F14201) at  $25^\circ\text{C}$  for 25 min. Fluorescence imaging (Zeiss Examiner Z1) was performed using an excitation light source of 470 nm (Colibri, Zeiss) for 2-4 min per recording frame area ( $692 \times 520$  pixels). Emitted light ( $\sim 515$  nm) was filtered (AHF, F66-422) and recorded via CCD camera to a PC at 12.5 Hz (Axiovision software). Imaging data was preprocessed by manual region-of-interest (ROI) pixel mapping and analysed with MEA activity in Matlab R2009b and OOCalc. Cells were classified functionally as neurons or as astrocytes according to their calcium transient onset kinetics and durations [4, 8].

### 2.3 MEA recordings

Electrical recordings were sampled at 25 KHz using Multichannel Systems software (MCRack, v3.8). Spike cutouts were generated by thresholding baseline activity at  $-5$  stdev. Bursts were detected offline in MCRack using the following interspike-interval (ISI) parameters: Max ISI to start burst, 60 msec; Max ISI to end burst, 120 msec; Min inter-burst interval, 300 msec; Min burst duration, 50 msec; Min no. spikes per burst,  $n = 5$ . Network bursts were defined in OOCalc as having: multi-site burst onsets occurring within 50 msec; and a minimum 3 site recruitment.

## 3 Results

### 3.1 $\text{Ca}^{2+}$ transients

28% (mean;  $\pm$  s.d. 18%) of the visible cells of a 22 DIV culture showed measurable changes in

calcium fluorescence, vs. 17% (mean; +/- 2% s.d.) for a 56 DIV culture. Two types of transient profiles were observed: fast onset (0.22 sec, mean; +/-0.15, s.d.) with relatively short duration (2.49 sec, mean; 1.18, +/- s.d.), i.e., consistent with neurons; and slower onsets (1.5 sec, mean; +/- 1.89, s.d.) with longer durations (7.83 sec, mean; +/- 5.64, s.d.), i.e., consistent with astrocytes.

### 3.2 Ca<sup>2+</sup> transients during bursts

Bursts in the 56 DIV culture occurred at a rate of 13.33 bursts/min with a mean 40 electrode recruitment, vs. 2.32 bursts/min across 30 electrodes in the 22 DIV culture. Neuronal Ca<sup>2+</sup> transients, irrespective culture age, were coupled to bursts with 97.7% coherence and by an average delay of 2.5 msec (+/- 98 msec s.d.). Glial Ca<sup>2+</sup> transients were often associated with bursts (76% coherence), but with greater variability in their relative onset times (-414.5 msec, mean; +/- 1.06 sec, s.d.). Burst duration did not predict neuronal Ca<sup>2+</sup> transient duration (RSq.<0.1), and was only a weak predictor for glial transient duration (RSq.=0.15).

### 3.3 Propagation patterns

Network burst propagation patterns consisted of several different motifs during each 2-4 min recording period (e.g., Fig. 1). Individual cell recruitment into network bursts was analysed using a Sørensen similarity index, yielding values ranging from 0.4 to 0.95. Duration of network burst, distance from burst origin to cells within the recording frame, and number of participating electrodes were not reliable predictors for the degree of similarity of individual cell recruitment (respectively, RSq. <0.1; RSq.=0.14; RSq.<0.1).

## 4 Discussion

Calcium transients were observed to be coupled to bursts in both neurons and glial cells, in both 22 and 56 DIV cultures. Whereas neuronal calcium transients showed well-defined onsets, coinciding with bursts, glial cell transient onsets were highly variable with respect to burst onsets. Slow Ca<sup>2+</sup> transient kinetics in these cells made it difficult to identify precise onset times, however. It is not yet clear under which conditions the greatest degree of coupling occurs between glial and neuronal Ca<sup>2+</sup> transients during bursts. However, there was an indication in neuronal cells at least that the number of participating electrodes depended on a common pool of 'initiator' sites within the culture recruiting other parts of the network; and provided that a minimum of three electrode sites were recruited then the level of

similarity in individual cell recruitment was relatively conserved.

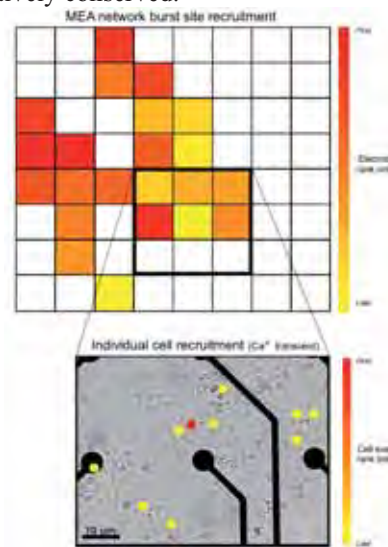


**Fig. 1.** A spontaneous propagation motif. Top: Schematic layout of MEA showing network burst propagation pathway by site recruitment order. Bottom: Optical recording frame (200x magnification) showing individual cell recruitment by calcium transient onset order within the optical recording frame.

### Acknowledgements

We thank Uni-Freiburg, the BCF, and IMTEK for the resources to carry out this research, as well U. Reide and P. Pauli for their assistance and culture preparations. Funding was provided by the German BMBF (BCCN Freiburg FKZ 01GQ0420 Freiburg\*Tübingen FKZ 01GQ0830).

### References

- [1] Opitz, T., Lima, A. D., Voigt, T. (2002): Spontaneous development of synchronous oscillatory activity during maturation of cortical networks in vitro. *Journal of Neurophysiology*, 88, 2196-2206
- [2] Smetters D., Majewski A., Yuste, R. (1999). Detecting action potentials in neuronal populations with calcium imaging. *Methods: A Companion to Methods in Enzymology*, 18, 215-221.
- [3] Regehr, W. G., Atluri, P. P. (1995): Calcium transients in cerebellar granule cell presynaptic terminals. *Biophysical Journal*, 68(5), 2156-2170
- [4] Ikegaya, Y., Bon-Jego, M. L., Yuste, R. (2005): Large-scale imaging of cortical network activity with calcium indicators. *Neuroscience Research*, 52, 132-138
- [5] Takayama, Y., Moriguchi, H., Kotani, K., Jimbo, Y. (2009): Spontaneous calcium transients in cultured cortical networks during development. *IEEE Transactions on Biomedical Engineering*, 56(12), 2949-2956
- [6] Wagenaar, D. A., Pine, J., Potter, S. M. (2006): An extremely rich repertoire of bursting patterns during the development of cortical cultures. *BMC Neuroscience*, 7(11), 1-18
- [7] Haydon, P. G. (2001): Glia: Listening and talking to the synapse. *Nature Reviews Neuroscience*, 2, 185-193
- [8] Takahashi, N., et al., (2007): Watching neuronal circuit dynamics through functional multineuron calcium imaging (fMCI). *Neuroscience Research*, 58, 219-225



## List of Authors

---

Aalto-Setälä K	122	Carrozzo M	336
Äänismaa R	90, 96	Casagrande S	47
Abad L	342	Cecchelli R	155
Abbracchio M	68	Cervello P	167
Agladze K	120	Chen Y	120
Alagapan S	191	Chiappalone M	62, 64, 145, 195, 197
Almog RO	277	Chichilnisky E	327
Ambard M	42	Choi I	279
Andruska A	227	Chong SA	58, 159
Aoyagi T	199	Chung Y	124
Arbuthnott G	207	Ciliberti D	303
Ashery U	74	Cipollone S	234
Atan S	124	Cismak A	247
Athias P	113	Colombo E	261, 295
Avenet P	167	Commisso E	193
Baaken G	251	Corner M	64
Bakker R	60, 183	Courtine G	229
Bakkum D	324, 340	Crofton K	149
Baldelli P	47, 157, 332	Crozes T	342
Baljon PL	78, 195, 283, 285	Dabrowski W	275, 327
Bartic C	58, 159	Damnjanovic S	147
Baumann W	66, 255, 289, 291, 293	D'Angelo P	145
Beggs J	275, 327	Dante S	47
Behrends J	251	Daus A	314
Beikrich H	291, 293	de la Paz F	223, 225
Benfenati F	47, 62, 145, 157, 281, 332	Decré M	303
Benilova I	159	Delattre V	40
Benito N	259	Deligkaris K	163
Ben-Jacob E	310	DeMaris A	76, 300
Berdondini L	47, 100, 175, 193, 332	DeMarse T	191, 216
Bertagnolli E	147	Destro-Filho JB	189
Bertrand D	167	DeStrooper B	159
Biffi E	187	DeWeerth S	212
Bikbaev A	38	Di Giovanni S	269
Bilbault JM	113	Diaz G	223, 225
Binczak S	113	Difato F	281
Biton B	167	Dihné M	86, 138
Blau A	281	Dimaki M	245
Boehler M	76, 227, 300	Dini P	42
Boido D	157	Dondapati S	251
Bologna LL	195	Dossi E	68, 70, 72
Bongard M	223, 225, 259	Drews G	305
Boren J	128	Düfer M	305
Boven KH	271	Dworak B	320
Bräunig P	257	Eberle W	58
Brewer G	76, 227, 300, 307, 320	Egert U	28, 42, 44, 51, 80, 220
Broersen K	159	Eglen SJ	100
Bröking K	253	Eickenscheidt M	222
Bugnicourt G	342	Einevoll G	170
Burkhardt C	218, 241, 267, 269	Elhady A	253
Callewaert G	58, 159	Elit J	267
Carabelli V	161, 261, 295	Erickson J	214
Carbone E	161, 261, 295	Eversmann B	331
Carrillo-Reid L	207	Farisello P	157
		Farrow K	106

Fernández E	223, 225, 259	Guvanasen G	212
Ferrández-Vicente J	223, 225	Haffner D	155
Ferrea E	157, 332	Hagner M	247
Ferrigno G	187	Hanein Y	263, 310
Fillafer C	147	Harbodt T	271
Fiscella M	106, 324	Harley C	78
Fischeneder M	147	Harris C	312
Fischer DC	155	Haeffner M	269
Fiutowski T	327	Heer F	340
Fleischer M	269	Heida T	49
Fournier T	342	Heikkilä J	90, 96
Franca E	191	Heilmann A	247
Franke H	68	Heine C	68
Frey U	106, 201, 324, 340	Heine M	38
Frischknecht R 3	8	Held J	241, 247, 291, 293
Fromherz P	46, 53, 174, 222, 331	Hembd C	271
Fuchsberger K	234, 267	Hennig MH	100
Fujiwara N	231	Herfurth P	261
Gabor F	147	Hermann C	46
Gabriel G	249, 259	Herrmann T	210, 220
Galneder R	271	Herzog N	263
Gambazzi L	234	Hescheler J	116, 126
Gandolfo M	100, 175, 195	Heuschkel M	316
Gao ZY	261, 295	Heynen J	241
Garcia-Munoz M	207	Hierlemann A	106, 201, 324, 340
Garofalo M	24, 193, 195	Hobbs J	275, 327
Gaspar J	247, 291, 293	Hoefler A	147
Gautam V	181, 287	Hogberg H	142
Gerber D	134	Homberg J	60
Gerling T	331	Hottowy P	275, 327
Gerwig R	267	Hufnagl M	147
Ghezzi D	157	Hynd M	318
Gibson H	134	Hyttinen J	92, 94, 122, 243
Gimsa J	66, 255, 289, 291, 293	Ide A	76, 227, 300
Giugliano M	40, 234, 316	Illes P	68
Gizurarson S	128, 130	Illes S	86, 138
Göbbels K	257	Imfeld K	157
Goddard M	80	Ingebrandt S	118
Godignon P	249	Ito D	20, 199
Gohara K	20, 199	Ito H	231
Goldhammer M	314	Jäckel D	106, 201
Gómez-Martínez R	259	Jacquir S	113
Gong XW	205	Jang MJ	279
Gong HQ	105, 205	Jepson L	327
Gosso S	161, 295	Jimbo Y	34, 54, 84, 88, 273, 309
Goto M	273, 309	Jing W	105
Goyal G	239	Joag C	216
Gramowski A	145, 151, 153, 155	Johnstone A	145, 149
Gritsun T	56	Jones I	106, 201
Gross G	145	Jones T	300
Grover M	212	Joye N	336, 338
Grybos P	334	Jügel K	151, 153, 155
Guenther E	116, 305	Kachel M	334
Guimerá A	249	Kachiguine S	327
Gullo F	68, 70, 72	Kanagasabapathi T	303
Gunning D	275, 327	Kandler S	28, 44
Guterman H	179	Kang G	239

Kang K	271	Liu JS	205
Kapucu FE	94	Liu L	102
Kauppinen P	243	Liu WZ	105
Kemenes I	312	Livi P	340
Kemenes G	312	Lorente V	223, 225
Kenney C	275	Lu QC	205
Kerkelä E	122, 265	Maccione A	47, 100, 175, 193, 195, 332
Kern D	269	Maffezzoli A	70, 72, 201
Khalid M	201	Magome N	120
Kibbel S	220	Maida S	187
Kim E	318	Mancuso S	346
Kim J	236	Marcantoni A	161, 295
Kim SJ	236, 318	Marconi E	47
Kiyohara A	231	Markram H	40, 234
Kmon P	334	Martin U	126
Koester P	66, 255, 289, 291, 293	Martin-Fernandez I	249
Kohn E	261, 295	Martinoia S	24, 62, 145, 175, 185, 189, 193, 195, 197
Komatsu T	20	Masi E	346
Korhonen I	92	Massobrio P	24, 185
Kotani K	54, 84, 88, 273, 309	Mathieson K	275, 327
Kötter R	60, 183	Mealing G	165
Krantis A	165	Men Y	261
Kraushaar U	116, 305	Menegon A	187
Krippeit-Drews P	305	Menzler J	104
Krylov S	277	Messa M	47
Kubon M	218	Mikkonen J	92, 94
Kudoh S	231	Miljanovic A	128, 130
Kujala V	122, 265	Misicka-Kesik A	153
Kunze A	316	Miwa K	34
Kuperstein I	159	Mönig N	28
Kuykendal M	212	Mori M	34
Lambacher A	174, 331	Moriguchi H	34, 54, 84, 88, 273, 309
Landry C	155	Moschallski M	218
Lanneau C	167	Moseler M	269
Larmagnac A	229	Mulas M	158
Laurent G	113	Müller J	106, 201, 324
Lavi A	74	Murr A	281
Law J	116	Musienko P	229
Le Feber J	30, 56, 64, 163	Nagarah J	78, 283, 285
Le Goff A	234, 267	Nam Y	236, 239, 279
Leblebici Y	336, 338	Narayan KS	181, 287
Lee JK	24	Narkilahti S	90, 92, 94, 96, 265
Lee S	236	Nguemo F	126
Lee W	218	Nieus T	175, 193
Lehmann M	126	Nisch W	218, 241, 269
Leibig C	108	Nomura M	299
Lekkala J	122, 243, 265	Noshiro M	34
Levenson J	134	Novellino A	142, 145
Levesque P	110	Offenhäusser A	257
Levin M	134	Okujeni S	28, 44, 51
Lewen G	110	Omerovic E	128, 130
Li Y	267	O'Shea M	312
Liang PJ	105, 205	Oury-Donat F	167
Lim J	239	Padberg A	220
Link G	218	Palomer X	249
Lipkowski A	153		
Litke A	275, 327		

Palosaari T	145	Shacham-Diamand Y	277, 297
Pan L	191, 307, 320	Shafer T	145, 149
Pasquale V	24, 62, 195, 197	Shao Y	128, 130
Pasquarelli A	161, 261, 295	Shein M	163, 310
Passaro P	312	Sheinin A	74
Pastewka L	269	Sher A	275, 327
Paul O	247, 291, 293	Shi H	110
Pearson R	76, 300	Shim W	124
Pedrocchi A	187	Shmilovich T	277
Peter C	147	Skoczen A	327
Petit M	342	Skottman H	90, 96
Pfeiffer T	118	Slippens T	60
Pietzka C	261	Sobanski T	142
Potter S	212	Sriperumbudur K	255
Prato M	234	Stamm B	269
Price A	142, 145	Stangl C	53
Rabner A	297	Stegenga J	49, 163
Ramunddal T	128	Stelzle M	218, 234, 267
Redon N	167	Stett A	210, 220, 241, 267, 269, 271
Regalia G	187	Stoyanova I	30
Reig R	249	Streichan R	106
Reimer T	66, 289	Stühmer W	253
Reinartz S	44	Stumpf A	241
Renaud P	316	Stürz K	116
Reppel M	116, 126	Suuronen R	90, 96
Rojo Ruiz J	161	Svendsen W	245
Roscic B	106	Sverdlov Y	277
Roska B	106	Szczygiel R	334
Rousseau F	159	Takahashi H	324
Rudd J	118	Takayama Y	54, 84, 88, 273, 309
Rühe J	251	Takeuchi A	34
Ruther P	247, 291, 293	Tamate H	20
Rutten W	30, 56	Tandeitnik P	179
Rydygier P	327	Tani H	34
Ryynänen T	122, 243, 265	Tanskanen J	94, 243
Saito At	84, 88, 273	Taub A	277, 297
Saito Ak	273, 309	Tauskela J	165
Sánchez-Vives M	249	Tautorat C	289, 291, 293
Scelfo B	145	Tedesco M	62, 145, 175, 193
Scheipers A	267	Theiss S	86, 138
Schlosshauer B	218	Thewes R	331
Schlüter O	253	Thielemann C	314
Schmid A	336, 338	Thivierge JP	165
Schnakenberg U	257	Toma F	234
Schneider K	269	Tourwe D	153
Schneider L	147	Urban G	218
Schneider M	261	van Leuven F	58
Schnitzler A	86, 138	van Ooyen A	257
Scholz B	218	van Wezel R	49
Schröder O	145, 151, 153, 155	Vandroux D	113
Schröder S	271	Varghese K	320
Schubert D	60, 183	Vazquez P	245
Schultz L	155	Villa R	249, 259
Schymkowitz J	159	Villard C	342
Sedivy J	201	Vitzthum V	174
Selten M	60, 183	Vörös J	229
Sernagor E	100		

Wagenaar D	78, 283, 285
Wang L	129
Wanke E	68, 70, 72, 201
Wanzenboeck H	147
Weihberger O	28, 51
Weiss D	151, 153, 155
Werner S	218
Wheeler B	76, 191, 216, 227, 300, 307, 320
Whelan M	145
Wirth M	147
Wolansky M	149
Wolf F	253
Wolff S	281
Wong P	124
Wüsten J	281
Xu B	113
Xu Y	295
Yang F	205
Yeung CK	118
Ylä-Outinen L	90, 92, 94, 96, 265
Yuan Q	120
Zeck G	104, 108, 174, 222
Zhang G	124
Zhang PM	105, 205
Zhu J	110
Ziegler C	281
Zoladz M	334
Zwanzig M	289



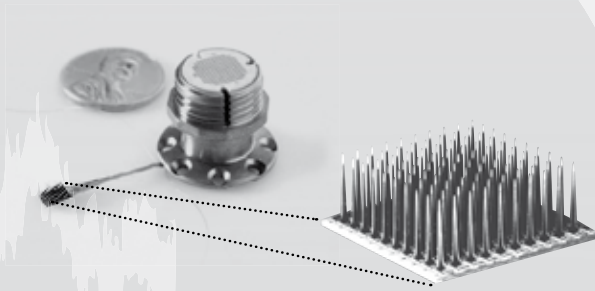




powered by  
**BLACKROCK**  
MICROSYSTEMS

# Utah Array: the best in the business ...

Today's standard for multichannel, high-density neural recordings from large populations of neurons\*



## ... make the best recordings:

Whether chronic or acute recordings  
Whether small or large subjects  
Whether slice or cell cultures

**Custom solutions for your research**

Blackrock Microsystems provides:

**Data acquisition systems**

>> High channel count

**Micro electrode arrays**

>> Various geometries

>> Multiple connectors



\* At the SfN 2009, nearly 75% of e-phys research papers referenced the Blackrock Microsystems' array (Utah Array).

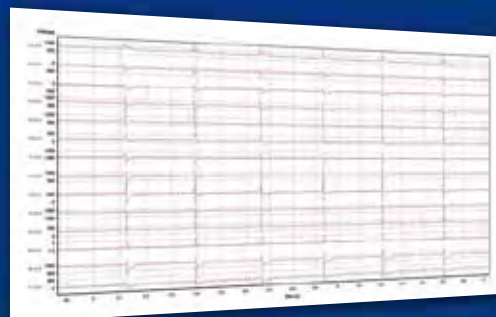
### BioMEA - Multi Electrode array

- 64, 128 or 256 independent channels
- Compact design
- Simultaneous acquisition and stimulation
- Compatible with inverted and upright microscopes
- Upgradeable to more channels
- High throughput multi-well capable
- Fully compatible with Ayanda Biosystems MEA

### User-friendly software interface

- Single control software for all functions
- Matlab interfacing. Spike2 compatible
- Full control of stimulation (no manual connections)
- Online and offline data treatment
- Visualization per well.
- Easy selection of electrodes

- Drug discovery and development
- Cardiac electrophysiology
- Retinal electrophysiology
- Acute Slices / Slice explant
- Cell cultures
- Neuroscience



Creative solutions  
for innovative laboratories

**BioLogic**  
Science Instruments

Bio-Logic SAS  
1, rue de l'Europe - F-38640 Claix - France  
Tél. +33 476 98 96 86 - Fax +33 476 98 69 09



Neurotechnology Research Systems

See us at booth #4

## Introducing the world's first high-resolution large-scale MEA platform

### BioCAM<sub>4096</sub><sup>TM</sup> by 3Brain

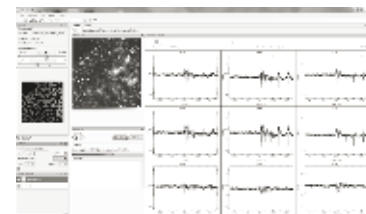
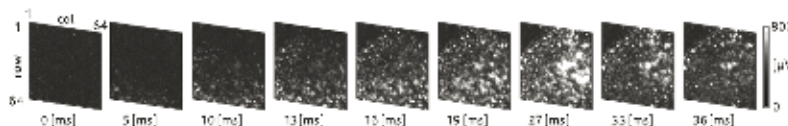
Complete system for high resolution in-vitro electrophysiology

- 4096 recording electrodes
- Electrode size: 21 μm x 21 μm
- Electrode separation: 21 μm
- Sensor area: 2.7 mm x 2.7 mm
- Real-time visualization as images or as conventional multichannel data
- Selectable regions of interest (ROI)
- Sampling rate: 8 kHz with 4096 electrodes, up to 90 kHz with ROI up to 64 electrodes
- Compatible size for mounting on microscope stages
- For use with all types of electrogenic tissue (neuron cultures, brain slices, cardiac tissue, etc.)
- Patented CMOS technology

BioCAM<sub>4096</sub> platform consists of:

1. APS<sup>®</sup> MEA NeuroChips
2. BioCAM<sub>4096</sub> Acquisition System
3. BrainWave Software

(\*) APS - Active Pixel Sensor



**KF Technology**

Life-Science Tools

**MED**  
systems<sup>™</sup>



**The MED64 multi-electrode array (MEA) system, based on planar micro-electrode array technology.** Simultaneous recording of extracellular signals across 64 channels without pulling glass electrodes.

**KF Technology Srl - Contact: Fabrizio Barbieri**

ph. (+39) 06 454.34.179 - info mobile: (+39) 339 533.03.22 Fax. (+39) 06 9725.3131-

SkyPe : kft2002 info@kftechnology.it [www.kftechnology.it](http://www.kftechnology.it)

**Laboratory Scientific Instruments - Life Sciences Systems**

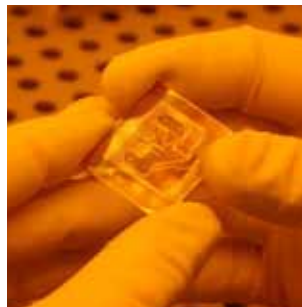
Products for Life Science research, Patch Clamp & Biological amplifiers, MEA System, Micromanipulators, Perfusion Systems, Electrophysiology equipment. Photometry, Imaging, Spectrofluorometers.



## MEAs are our passion >>

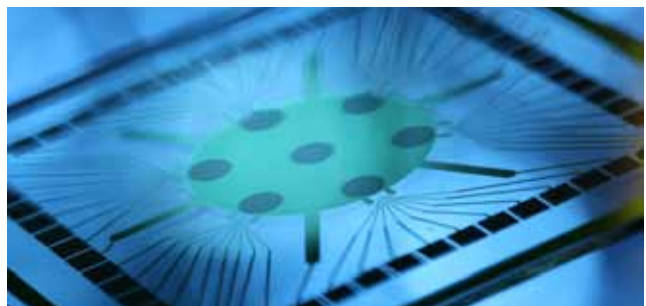
NMI Natural and Medical  
Sciences Institute at  
the University of Tübingen

With engineering experience gathered in more than 20 years, we develop and fabricate microelectrode arrays for scientific applications in neuroscience, cardiovascular research and neurotechnology.

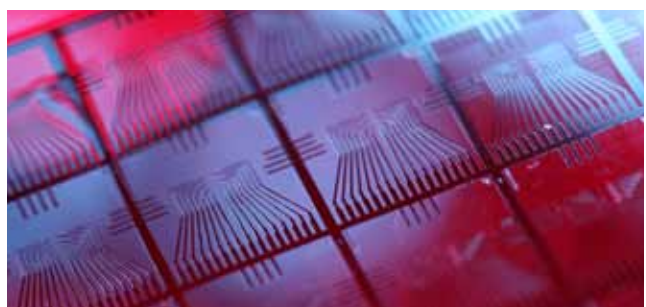


## >> Our passion is your benefit

- Application-specific designs on glass and polyimide for *in vitro* and *in vivo* electrophysiology,
- high-quality arrays with surfaces and electrodes applied and validated by hundreds of scientists,
- short time-to-application by routine fabrication of small batches of tailored designs,
- assured delivery of arrays at constant quality in numbers matching your needs,
- layouts and electrode performance fully compatible to the Multi Channel Systems MCS hardware.



## >> Benefit from your own MEA!



**Contact**  
mea@nmi.de

**NMI**  
Markwiesenstr. 55  
72770 Reutlingen, Germany



# MEA\*

## Need a recording system for your MEA?

### Acute hippocampal slice recording system:

This system is a stand-alone solution for extracellular recording and stimulation with perforated MEAs. It contains a 32 channel amplifier and data acquisition, as well as a four channel current stimulator. Up to four units can be operated independently from one computer.

### 256 channels for recording and stimulation:

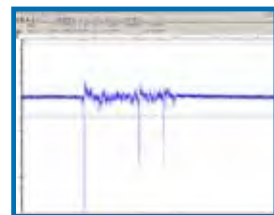
All necessary components are combined in one device. With the high number of electrodes you can cover a large area to record from different spots on your preparation and have a better spatial resolution of the signal propagation. Now available: 256MEAs with 60  $\mu\text{m}$  spacing and 10  $\mu\text{m}$  diameter.

### Real-time signal detection and feedback:

By moving the analysis from the PC to the DSP (Digital Signal Processor) integrated in the USB data acquisition hardware, a real-time signal detection/feedback is possible. The real-time signal detection/feedback is an advantageous feature if you need fast and predictable reactions related to recorded analog signals without time delay.

### Latest development:

Come to our booth and see the latest prototype of our MEA-Systems. It features more than 100 channels with integrated stimulation for each channel and includes advanced stimulus artefact suppression. The gain can be selected by software. A broadband filter amplifier for spike and slow field potential recordings completes the system.



[www.bio-pro.de](http://www.bio-pro.de)

ISBN-13 978-3-938345-08-5



BIOPRO Baden-Württemberg GmbH · Breitscheidstraße 10 · 70174 Stuttgart/Germany  
Phone +49 (0) 711 218 185 00 · Fax: +49 (0) 711 218 185 02 · E-Mail: [info@bio-pro.de](mailto:info@bio-pro.de)